



## BIROn - Birkbeck Institutional Research Online

Rixhon, G. and Briant, Rebecca M. and Cordier, S. and Duval, M. and Jones, A. and Scholz, D. (2017) Revealing the pace of river landscape evolution during the Quaternary: recent developments in numerical dating methods. *Quaternary Science Reviews* 166 , pp. 91-113. ISSN 0277-3791.

Downloaded from: <https://eprints.bbk.ac.uk/id/eprint/16009/>

*Usage Guidelines:*

Please refer to usage guidelines at <https://eprints.bbk.ac.uk/policies.html>  
contact [lib-eprints@bbk.ac.uk](mailto:lib-eprints@bbk.ac.uk).

or alternatively

1 **Revealing the pace of river landscape evolution during the Quaternary: recent**  
2 **developments in numerical dating methods**

3

4 *Gilles Rixhon, Rebecca M. Briant, Stéphane Cordier, Mathieu Duval, Anna Jones, Denis Scholz*

5

6 *Abstract*

7 *During the last twenty years, several technical developments have considerably intensified the use of*  
8 *numerical dating methods for the Quaternary. The study of fluvial archives has greatly benefited from*  
9 *these enhancements, opening new dating horizons for a range of archives at distinct time scales and*  
10 *thereby providing new insights into previously unanswered questions. In this contribution, we*  
11 *separately present the state of the art of five numerical dating methods that are frequently used in the*  
12 *fluvial context: radiocarbon, Luminescence, Electron Spin Resonance (ESR), <sup>230</sup>Th/U and terrestrial*  
13 *cosmogenic nuclides (TCN) dating. We focus on the major recent developments for each technique*  
14 *that are most relevant for new dating applications in diverse fluvial environments and on explaining*  
15 *these for non-specialists. Therefore, essential information and precautions about sampling strategies*  
16 *in the field and/or laboratory procedures are provided. For each method, new and important*  
17 *implications for chronological reconstructions of Quaternary fluvial landscapes are discussed and,*  
18 *where necessary, exemplified by key case studies. A clear statement of the current technical*  
19 *limitations of these methods is included and forthcoming developments, which might possibly open*  
20 *new horizons for dating fluvial archives in the near future, are summarised.*

21

22 **Keywords:** numerical dating method, fluvial archives, Quaternary, <sup>14</sup>C dating, Luminescence dating,  
23 ESR dating, <sup>230</sup>Th/U dating, terrestrial cosmogenic nuclides dating

24

25 **1. Introduction**

26 Unravelling processes and rates of long-term landscape evolution, focusing on the evolution of river  
27 drainage systems, has been a core topic in the earth surface sciences since Davis's (1899) pioneering  
28 work more than a century ago. Since then, river terrace sequences and/or related landforms have thus

29 been extensively used as geomorphic markers across the world. However, assigning chronologies to  
30 these sequences and related river sediments or landforms has constantly been challenging. Until the  
31 late 20<sup>th</sup> century, this goal was often achieved using diverse methods that provide relative age  
32 information on Quaternary fluvial deposits. Such methods included: correlation with the alpine glacial  
33 chronology (e.g. Brunnacker et al., 1982), soil chronosequences (e.g. Engel et al., 1996),  
34 palaeomagnetism (e.g. Jacobson et al., 1988), clast seismic velocity (e.g. Crook, 1986), weathering  
35 rind analysis (e.g. Colman & Pierce, 1981), obsidian hydration (e.g. Adams et al., 1992), amino-acid  
36 racemization of terrestrial molluscs (e.g. Bates, 1994) or correlation to Marine Isotope Stages (MIS)  
37 via mammalian (e.g. Schreve, 2001) and molluscan (e.g. Preece, 1999) biostratigraphy. Combining  
38 these methods often yielded insightful relative chronologies for Quaternary terrace flights (e.g.  
39 Knuepfer, 1988; Schreve et al., 2007).

40 Whilst methodological improvements to some of these techniques have since been achieved (e.g.  
41 Penkman et al., 2007 for amino-acid racemization), in most instances, relative dating methods have  
42 been progressively supplemented by dating methods delivering absolute numerical ages over the last  
43 two or three decades. With the exception of radiocarbon dating, which has been applied since Libby's  
44 seminal paper (Libby et al., 1949), the development of most of these geochronometers occurred in  
45 relation to major theoretical and/or technical improvements in the late 20<sup>th</sup> century. For instance,  
46 although cosmic rays were discovered in 1912 by the Nobel laureate Victor Hess, only the  
47 development of accelerator mass spectrometers (AMS) in the 1980s enabled measurements of  
48 cosmogenic nuclide concentrations (e.g. Klein et al., 1982) and thus their use as a geochronometer  
49 (e.g. Nishiizumi et al., 1986). Likewise, Electron Spin Resonance (ESR) spectroscopy, already  
50 outlined in the mid 1930s (Gorter, 1936), was first successfully applied as a dating tool only 40 years  
51 later (Ikeya, 1975).

52 In the framework of this FLAG (Fluvial Archives Goup) special issue, we present and discuss the  
53 recent major dating advances offered by modern numerical methods in diverse fluvial environments.  
54 Five methods are discussed: radiocarbon, Luminescence, Electron Spin Resonance, <sup>230</sup>Th/U and  
55 terrestrial cosmogenic nuclide (TCN) dating. They were specifically selected amongst the array of  
56 Quaternary dating methods because (i) they are commonly used in the fluvial context, (ii) they have all  
57 experienced major theoretical and/or technical developments during recent decades, (iii) they require  
58 different dateable material and thereby may also yield information about a wide range of fluvial  
59 processes and environments, (iv) they have different time ranges of application, but altogether, span

60 the last million years (Fig. 1). Detailing all theoretical principles of the individual techniques is beyond  
61 the scope of this contribution. Instead, the focus is on relevant major technical developments and how  
62 these enabled new dating applications for different kinds of fluvial archives in distinct settings. The  
63 pathways of dateable material within fluvial systems are detailed in Figure 2. Fundamental information  
64 and precautions about sampling strategies in the field and/or laboratory procedures are also provided.  
65 Whilst these are well known by geochronologists, they have not often been published and need  
66 therefore to be clarified to non-specialists who intent to collect samples for dating. For each method,  
67 new and important implications for chronological reconstructions of Quaternary fluvial landscapes are  
68 also discussed and, if necessary, exemplified. Case studies published in outputs related to former  
69 FLAG activities and using one (or more) of these dating method(s) are listed in Table 1. Current  
70 technical limitations and probable forthcoming developments are also addressed.

## 71 **2. Radiocarbon dating of fluvial deposits**

72 Radiocarbon dating has been a common method applied to fluvial deposits in those settings where  
73 organic material is readily preserved within sequences, i.e. partially or fully waterlogged parts of the  
74 floodplain system, including channels and overbank deposits (Fig. 2). As a technique it has  
75 contributed significantly to understanding key questions, both about palaeoenvironmental information  
76 contained within fluvial deposits (e.g. Kasse et al., 1995) and about periods of river activity (e.g.  
77 Macklin et al., 2005). The accuracy with which age estimates can be gained from ever smaller  
78 samples has improved significantly over the 60-70 years since the first development of the technique.  
79 This is partly due to the increasingly routine use of accelerator mass spectrometry (AMS)  
80 measurements of smaller samples (~1 mg in some cases, Ruff et al., 2010, but more robustly 5-6 mg,  
81 Brock et al., 2010). Another important development has been the significant international cooperation  
82 involved in calibrating radiocarbon measurements against independent annually-resolved records to  
83 account for natural variability in the concentration of atmospheric  $^{14}\text{C}$ , culminating most recently in the  
84 IntCal13 dataset (Reimer et al., 2013).

85 The  $^{14}\text{C}$  dating method can be applied to any material that contains carbon. This includes: cellulose-  
86 containing materials (wood, seeds, plant remains), charcoal and charred material, carbonates  
87 (including corals, foraminifera, shells), collagen-containing materials (bone, tooth, antler, ivory), hair,  
88 and bulk sediment. Many of these are found within fluvial deposits in more temperate environments,  
89 where preservation conditions are favourable, but not all are *in situ* (Fig. 2). Therefore, when

90 considering the radiocarbon dating of fluvial deposits, we need to consider the issue of provenance  
91 and reworking. In addition, calibration, reservoir effects and appropriate pretreatments are also  
92 relevant to fluvial archives in lakes, but reviewed elsewhere (Brauer et al., 2014).

93 All present-day carbon-bearing material contains three naturally occurring carbon isotopes. Of these,  
94  $^{14}\text{C}$  is radioactive, with a half life of  $5730 \pm 40$  years (Godwin, 1962). The source of this  $^{14}\text{C}$  is cosmic  
95 ray activity in the atmosphere. This enters the global carbon cycle when it is oxidised to  $\text{CO}_2$ , and  
96 concentrations are very low compared to  $^{12}\text{C}$  and  $^{13}\text{C}$ . Conventional radiocarbon ages are calculated  
97 from measured concentrations of  $^{14}\text{C}$ , using either beta counting methods or, meanwhile more  
98 commonly, AMS. To allow consistency with earlier analyses, these are reported using the original  
99 Libby half life of 5568 years (e.g. Stuiver and Polach, 1977; Reimer et al., 2004). They are also  
100 corrected for fractionation processes that occur during measurement, as described by Brauer et al.  
101 (2014). Because of the multiple stages at which differences can occur within the calculation of a  
102 radiocarbon age, they should be reported in detail according to the conventions described by Millard  
103 (2014).

#### 104 *2.1. Provenance and reworking of radiocarbon samples in the fluvial environment*

105 A feature of fluvial systems is the wide range of depositional environments which may be found within  
106 a single catchment, including, for instance, river channel, floodplain and floodbasin deposits. These  
107 differ in frequency of depositional events, deposited grain sizes and likely presence of *in situ* organics  
108 (Fig. 2). The nature and rate of fluvial activity within a reach determine the spatial distribution of  
109 depositional environments and their preservation within the alluvial record (Lewin and Macklin, 2003).  
110 The depositional context of a radiocarbon-dated sample determines its suitability for answering  
111 questions about the timing of events within a fluvial system. Where possible, a distinction should  
112 therefore be made between radiocarbon dates from within thick sedimentary units and those collected  
113 at or close to boundaries between units. The former provide a single age for processes, such as  
114 vertical sediment accretion or lateral channel migration, operating over an extended time period  
115 (Lewin et al., 2005), while the latter constrain the timing of events in the river system that produced  
116 sedimentological changes (Macklin and Lewin, 2003). In Late Pleistocene to Holocene settings, where  
117 detailed sedimentological information is more commonly preserved, radiocarbon dates on fluvial units  
118 have been classified as river activity ages, in minerogenic sediment, or river stability ages, on peat or  
119 palaeosols (Zielhofer and Faust, 2008). Sedimentary units indicative of river activity and river stability

120 may be produced simultaneously in different depositional environments within a single reach (Zielhofer  
121 and Faust, 2008). Radiocarbon dates close to sediment unit boundaries provide maximum or  
122 minimum ages for events which produced features such as reversals in fining upwards sediment  
123 sequences or renewed fluvial sedimentation above a peat or palaeosol (Macklin et al., 2005).  
124 Radiocarbon-dated samples from a unit directly below such a sedimentological change, giving a  
125 maximum age ('change after' dates), are regarded as the most reliable indicator of the age of the  
126 event which produced the change in sedimentation rate or grain size (Macklin et al., 2010). In older  
127 deposits, where fewer units are amenable to radiocarbon dating, such precise analysis of how the  
128 dates relate to fluvial activity is less feasible. Nonetheless, the sedimentological setting should be  
129 assessed in a similar way so that the age estimate obtained can be most effectively interpreted. In  
130 addition, care should be taken to interpret the different transport pathways of the type of material to be  
131 dated.

132 Further to their diversity, river catchment systems are highly dynamic and material can be transported  
133 varying distances from the original source. It can also be kept in storage on hillslopes or within  
134 floodplains and released into the channel tens to thousands of years afterwards (Fig. 2). Therefore,  
135 when radiocarbon dating material from fluvial deposits, the possibility of reworking must always be  
136 borne in mind. This can be especially problematic in relation to carbon-bearing material that does not  
137 easily break down in transport (Fig. 2), for example wood, bone and some shells (either because they  
138 are calcitic, such as shell opercula, or because they are light and travel in suspension rather than  
139 bedload). Therefore, it is essential to date only the identifiable fraction of the deposit (Table 2). In  
140 addition to being identifiable, it is necessary to exercise common sense over how likely the material  
141 isolated is to have been contemporaneous with deposition (e.g. not choosing material suggesting a  
142 temperate climate if preserved within cold stage deposits).

## 143 *2.2. Calibration*

144 Due to natural variability in cosmic ray production and exchange between different carbon stores (i.e.  
145 ocean, terrestrial ecosystems and atmosphere) the concentration of  $^{14}\text{C}$  in the atmosphere varies over  
146 time. For this reason, to convert radiocarbon ages to calendar ages, a detailed calibration curve has  
147 been constructed from independently dated (often annually resolved) records including tree-rings,  
148 varves, corals and speleothems. The tree-ring curve extends to 13,900 cal years BP (Reimer et al.,  
149 2013) and is the most robust part of the curve. The extension beyond this to 50,000 cal years BP is

150 based on multiple datasets which diverge from each other in places, creating larger errors. The  
151 radiocarbon community meets regularly to review this curve and the most recent data set is IntCal13  
152 (Reimer et al., 2013) – or SHCal13 for the Southern Hemisphere (Hogg et al., 2013), which is now  
153 included in all calibration software (e.g., CALIB, OxCal, BCal). The output of calibration is an interval  
154 of possible calendar ages that correspond to the  $^{14}\text{C}$  age calculated from the measured  $^{14}\text{C}$   
155 concentration. Often multiple intervals correspond to the measured concentration.

### 156 2.3. Freshwater reservoir effects and radiocarbon dating of fluvial archives

157 When dating plant or shell material, the preferred habitat of the species used is crucial. If the material  
158 to be dated is from an aquatic species, the chemistry of the water body must be taken into account.  
159 The presence of 'old carbon' which is 'dead' with respect to radiocarbon can lead the  $^{14}\text{C}$  of the water  
160 to have an apparent age. This apparent age is then transferred to the material being dated. This issue  
161 has been known for many years, with very early studies showing that *Potamogeton*, an aquatic plant  
162 which is believed to photosynthesise within the water column, yielded an apparent age in modern  
163 hardwater lakes of ~2000 years (Deevey et al., 1954). For this reason, the first choice of material to  
164 date would instead be a plant which photosynthesises directly with the atmosphere such as *Scirpus* or  
165 *Carex* (Deevey et al., 1954).

166 Determining the freshwater reservoir effect in lakes (where some fluvial archives are found) is based  
167 on the assumption that the effect has remained constant and can be corrected for. In relation to rivers,  
168 this is more problematic because most studies (e.g. Deevey et al., 1954) have been carried out in  
169 lakes. A recent study (Philippsen, 2013) of water, plants and animals from rivers in northern Germany  
170 showed significant temporal variability in the scale of reservoir age in both the dissolved inorganic  
171 carbon (DIC) from river water itself (a range of 1527-3044 years) and the reservoir age in aquatic  
172 plants (a range of 350-2690 years). Of particular interest is the finding that the radiocarbon values  
173 from river water are directly related to the balance between groundwater and precipitation inputs to the  
174 system. When precipitation was higher before samples were taken, associated radiocarbon reservoir  
175 ages of river water were younger. This means that the freshwater reservoir effect in fluvial deposits is  
176 likely to be present, but to varying degrees. The main way to avoid this issue is to date only terrestrial  
177 species of plants or molluscs (Table 2), which requires the investigator to develop some skills in fossil  
178 identification. Brauer et al. (2014, p.49) recommend for lake or speleothem sequences that where  
179 samples known to be affected by a freshwater reservoir effect have been measured, these "must be

180 corrected prior to calibration by subtraction of the age offset estimated using the measured  $^{14}\text{C}$   
181 concentration of known age samples". In the fluvial setting, given the demonstrable variability in  
182 freshwater reservoir effect in relation to discharge, and the known large fluctuations in discharge  
183 regime over the time period of the radiocarbon technique, this is unlikely to be possible. The  
184 radiocarbon dating of aquatic species should therefore be avoided unless a 2000 year uncertainty is  
185 sufficient to answer the research question being posed.

#### 186 *2.4. Laboratory pretreatments*

187 Because the concentrations of  $^{14}\text{C}$  are so low in materials used for radiocarbon dating, the possibility  
188 of contamination with modern carbon is always present. Contamination during sample preparation can  
189 be avoided as detailed in Table 2. Removing contamination that has accumulated *in situ* requires  
190 laboratory pretreatment (Table 2) and becomes more crucial for samples near the limit of the  
191 radiocarbon technique between 30,000-50,000  $^{14}\text{C}$  years BP, because the amount of  $^{14}\text{C}$  present  
192 within the sample is so low that any contamination has a much larger effect (Fig. 3). This is particularly  
193 important in many discontinuous fluvial sequences where problems with dating cannot be detected in  
194 the context of a vertical sequence.

195 Significant progress has been made in recent years in providing more reliable radiocarbon ages on  
196 bone and charcoal from this older time period (e.g. Higham et al., 2006; Bird et al., 1999) and these  
197 pretreatments should be used for these materials. However, fluvial sequences sometimes lack these  
198 dating materials, which are best preserved in dry, alkaline conditions (the opposite of the wet, acidic  
199 conditions often present in fluvial systems for the preservation of environmental material). There are  
200 as yet no 'stand-out' preferred pretreatments for the shell or seed material more commonly preserved  
201 in fluvial deposits, and advice should be sought from the radiocarbon laboratory with which you are  
202 working if the samples are likely to be near the limit of the technique.

### 203 **3. Luminescence dating of fluvial deposits**

204 The Optically Stimulated Luminescence (OSL) dating method is currently one of the most commonly  
205 applied to fluvial sediments because it directly dates the sand/silt grains of which such sediments are  
206 often composed. These grains enter the river system from hillslopes and then travel in suspension  
207 through the fluvial system, passing into and out of storage before final deposition (Fig. 2). This method  
208 was developed during the 1980s as an alternative to Thermoluminescence (TL). It became widely  
209 used ~15 years ago, in particular due to the development of the Single Aliquot Regenerative (SAR)

210 protocol (Murray and Wintle, 2000; 2003) which replaced previous additive approaches. The SAR  
211 protocol enables multiple age estimates to be measured from a single sample, generating more  
212 accurate final ages (Duller, 2008). Continuous improvements to precision and accuracy have occurred  
213 during past decades, giving the OSL method a key role in the dating of Quaternary fluvial archives.  
214 Many publications in special issues of the FLAG include an OSL-based geochronological approach  
215 (Table 1). Questions that have been answered by using this approach encompass, for example, the  
216 timing of phases of fluvial activity in relation to climate (e.g. Briant et al., 2004) or the dating of terrace  
217 bodies associated with archaeology (e.g. Cunha et al., 2012; this issue/2016).

218 Several relevant reviews related to the technical details of optical dating of fluvial deposits have been  
219 published (e.g. Wallinga, 2002; Rittenour, 2008), so the principles and basic procedures are here only  
220 briefly mentioned. Instead, we focus particularly on what researchers working on fluvial archives need  
221 to know to successfully apply this method to their samples. This includes sampling strategies, new  
222 protocols and statistical treatment of data required to derive reliable age estimates.

223 The OSL method is based on the estimation of the impact of radiation on the crystalline structure of  
224 minerals such as quartz and feldspar while they are shielded from light (e.g. Duller, 2004). The  
225 radiation ( $\alpha$ ,  $\beta$ ,  $\gamma$ ) comes from radionuclides which are present in the mineral and its natural  
226 environment, mainly U, Th (and their decay products) and K, with a small proportion from cosmic  
227 particles. This radiation leads to the trapping of electrons in crystalline lattice defects. The total amount  
228 of trapped electrons within a crystal is proportional to the total energy (dose) absorbed by the crystal,  
229 which naturally increases with time. As soon as the mineral is exposed to sunlight, especially during its  
230 transport, trapped electrons are released from the traps. This generates the emission of light (the  
231 luminescence signal) which can be measured following light stimulation (Huntley *et al.*, 1985). The age  
232 of the sediment is then estimated by dividing the  $D_E$  (equivalent dose) by the dose rate (the rate at  
233 which the sediment is exposed to natural radiation).

234 It should be noted that the sensitivity of mineral grains to optical stimulation is highly variable, making  
235 some depositional settings inherently more successful than others. "Quartz grains that have  
236 undergone repeated cycles of bleaching and deposition tend to become sensitized ... and so for some  
237 samples a large fraction of quartz grains will yield a measurable OSL signal... [In contrast], samples  
238 from any environment can show poor sensitivity and highly-skewed sensitivity distributions ...[where]...  
239 95% of the combined OSL signal comes from less than 5% of the grains" (Cunningham and Wallinga,  
240 2012, p.17). In addition, the commonly-used SAR protocol may not be applicable for all samples.

241 Standard tests for the appropriateness of the SAR protocol include the use of a dose response test  
242 (i.e. can the laboratory protocol successfully remeasure a known dose?) and the recycling ratio (i.e.  
243 does the test dose successfully correct for sensitivity changes during measurement?). However,  
244 recent experimental work suggests that these may be insufficient tests (Guerin et al., 2015; Timor-  
245 Gabar et al., 2015). It is possible that this is due to an initial sensitivity change that is not corrected for  
246 by the use of the response to a test dose.

### 247 *3.1. Causes of age underestimation*

248 The complexities involved in generating a luminescence signal mean that in some cases it is not  
249 possible to provide a reliable age determination, either over- or under-estimating the age of the  
250 sediment. Underestimation may occur when the mineral is saturated. This means that all traps have  
251 been filled with electrons, thus preventing additional trapping. The measured signal will hence only  
252 reflect a part of the burial duration, and the obtained age must be considered as a minimum age.  
253 Saturation explains why the OSL method cannot be applied to old sediments. The age limit varies  
254 between minerals, but quartz often saturates at doses of ~200-300 Gy (Table 3, Wintle and Murray,  
255 2006). This makes it difficult to date sediments beyond 150 ka (except when the dose rate is quite  
256 low).

257 Feldspars in contrast saturate at higher doses and may in theory be used to date Middle Pleistocene  
258 sediments (Table 3). However, feldspars are affected by anomalous fading. This is the spontaneous  
259 eviction of electrons from deep traps without light stimulation (Wintle, 1973) which can then lead to  
260 age underestimation. Several procedures have been developed to detect and correct for anomalous  
261 fading by estimating fading rates (Huntley and Lamothe, 2001). Another approach is the post-IR-IRSL  
262 procedure (Thomsen et al., 2008). This procedure is based on the measurement of an elevated  
263 temperature (>200°C) post-IR IRSL signal immediately after the IRSL measurement (typically  
264 performed at 50 °C). The post-IR IRSL signal is characterised by a higher stability and thus yields  
265 lower fading rates (Buylaert et al., 2009). However, the post-IR IRSL signal is harder to bleach than  
266 the IRSL signal.

### 267 *3.2. Fluvial transport and incomplete bleaching: a main source of age overestimation*

268 The physical principles behind OSL suggest that the method is well suited to the study of fluvial  
269 sediments, since it allows direct dating of the last transport-and-sedimentation process (Table 3).  
270 However, in addition to the mineral-related issues described above, a key issue related to the dating of

271 fluvial sediments is the potential occurrence of incomplete bleaching. This phenomenon occurs when  
272 grains have not been exposed to sufficient daylight during transport. In this case, a part of the  
273 measured OSL signal is formed by electrons that remained trapped despite the fluvial transport  
274 (inherited component; Murray and Olley, 2002). This leads to an overestimation of the age, which is  
275 significant in the case of young sediments (less than 2 ka; Jain et al., 2004), but may also affect older  
276 sediments. For this reason, the detection and avoidance of incomplete bleaching is fundamental to  
277 obtain reliable burial ages to infer the timing of deposition.

278 In the case of fluvial sediments, these should be selected for sampling to maximise bleaching in the  
279 depositional setting. The degree of bleaching of the individual grains depends on two main parameters  
280 (Stokes et al., 2001): transport length, and the transport conditions. Sufficient transport is necessary to  
281 ensure complete bleaching of the signal. Studies focusing on transport length showed that the  
282 inherited signal was significantly reduced after a transport of several tens or hundreds of km (Murray  
283 and Olley, 2002). The second parameter refers to the way the grains are transported and includes,  
284 amongst others, the water turbidity and the channel depth. Grains that have been transported in a  
285 deep water column (leading to strong attenuation of the solar spectrum) and/or in turbid water may  
286 therefore be incompletely bleached (e.g. Ditlefsen, 1992). Settings in which samples are more or less  
287 likely to be completely bleached are represented in Figure 2. However, the expertise of the researcher  
288 must be employed at the site to truly maximise the likelihood of sampling completely bleached  
289 material, since the presence of turbid water or a deep water column will usually leave a sedimentary  
290 signature.

### 291 *3.3. The importance of the sampling strategy*

292 Following from this, the sampling strategy should aim to collect the potentially best bleached grains,  
293 keeping in mind that the OSL method is mainly applied to sand- (100-250  $\mu\text{m}$ ) or silt- (4-11  $\mu\text{m}$ ) sized  
294 grains. This makes it necessary to perform fine sedimentological investigations to interpret the  
295 depositional locations (i.e. channel/palaeochannels, point bar, crevasse splay, floodplain deposits).  
296 Most sediments analysed to date have been collected in channels or point bars (Figs. 2&4), as these  
297 are more clearly associated with significant transport of the grains. OSL dating of floodplain deposits is  
298 less common, but possible especially in the case of sandy facies (Keen-Zebert et al., 2013).  
299 Considering the sedimentation process is also very important, as the exposure to sunlight will be  
300 different in a flood dominated river (typical of Mediterranean or semi-arid areas) or a less ephemeral  
301 river. In the latter, presence of a more regular water flow will allow grains to be more completely

302 bleached, while in the former case mass transport associated with floods may prevent complete  
303 zeroing (Bartz et al., 2015).

304 In common with all depositional locations, the sampling should ideally be performed in thick (>30 cm  
305 both above and below the sample) homogeneous layers, to ensure that the dose rate estimation is as  
306 simple as possible (Fig. 4a). This is particularly important if the field scientist does not have access to  
307 a field gamma spectrometer which can capture the dose rate from this full radius of gamma radiation  
308 (Fig. 4b). In the common case of a thinner bed surrounded by inhomogenous sediments, detailed  
309 attention should be paid to the 'micro-stratigraphy' and small samples for laboratory dose rate  
310 measurement taken from all sediment types within a 30 cm radius of the sample. These can have  
311 significantly different dose rates (clays are often higher, gravels lower) and this can be adjusted for  
312 using the methods published by Aitken (1985) if such samples are taken. It is worth being aware,  
313 however, that the greater complexity of dose rates and lower likelihood of complete bleaching may  
314 make the results from such samples hard to interpret.

315 The choice of the mineral to be studied as a dosimeter is also crucial, if a choice is possible. Both  
316 theoretical work and comparative analyses by Wallinga et al. (2001) showed for Upper Pleistocene to  
317 Holocene sediments that quartz was a preferred dosimeter. The quartz grains are more rapidly  
318 bleached than feldspars (a few seconds vs a few tens of seconds, Huntley et al., 1985), and not  
319 affected by anomalous fading. For older deposits, trade offs must be made, and feldspars may be  
320 selected to allow dating of older deposits, with anomalous fading effects taken into account and  
321 corrected for as well as possible.

322 This sedimentological approach is fundamental in selecting the grains with the best properties for  
323 dating. However, it may in some cases not be sufficient to avoid heterogeneous bleaching. There are  
324 measurement protocols that seek to avoid partial bleaching by measuring or reporting only the well-  
325 bleached component within a sample (e.g. 'early background subtraction', Cunningham and Wallinga,  
326 2010, or combined IR and OSL stimulation, Jain et al., 2005). However, none of these methods have  
327 become mainstream approaches as yet. It is also worth noting that field investigations and sampling  
328 may benefit from the use of recently developed portable readers (Sanderson and Murphy, 2010).  
329 These make it possible to broadly estimate luminescence intensities and, when combined with *insitu*  
330 gamma spectrometry, the depositional age. Whilst the precision is too low for this to replace laboratory  
331 measurements, it may be a useful tool in the case of complex depositional patterns, to detect

332 potentially problematic samples and guide sampling strategies (Stone et al., 2015). It has yet to be  
333 tested on fluvial sediments, or at the lower luminescence intensities typical of temperate-zone  
334 samples.

335 *3.4. Detection of incomplete bleaching during OSL measurements and statistical treatments to*  
336 *address this issue*

337 Incomplete bleaching can be detected while performing luminescence measurements in the  
338 laboratory. Large-scale assessments can be made firstly by measuring both quartz and feldspars for a  
339 given sample. As the dosimeters have different bleaching rates, obtaining comparable ages provides  
340 evidence for complete zeroing of the sediments prior to burial (Colarossi et al., 2015). The testing of  
341 modern analogues (recent sediments transported under conditions similar to those under study) may  
342 also be useful (e.g. Geach et al., 2015), provided such sediments are available.

343 It is possible to statistically separate different parts of the luminescence signal to isolate the 'fast'  
344 component, which is most easily bleached (e.g. Singarayer and Bailey, 2004). The most common way  
345 of detecting incomplete bleaching in the laboratory, however, is through investigation of the distribution  
346 of multiple age estimates from a sample. The SAR protocol is based on the measurement of multiple  
347 equivalent doses (from aliquots or single grains) for a given sample. The number of aliquots used  
348 varies, but Rodnight (2008) proposed 50 aliquots as a minimum based on analysis of a poorly  
349 bleached fluvial sample. In some case higher values are required or lower may be sufficient (Galbraith  
350 and Roberts, 2012). It is important that these measurements are performed on small aliquots or single  
351 grains to avoid averaging of the signal across the aliquot.

352 The initial assumption is that a fully bleached sample will yield consistent  $D_E$  values (excluding  
353 analytical uncertainty). Therefore, the presence of scattering in the  $D_E$  distribution is taken as an  
354 indication that some aliquots have been incompletely bleached. Whilst this is commonly represented  
355 as a histogram or probability density function, recently many workers have started to use radial plots  
356 which allow the inclusion of information on the precision of each  $D_E$  (e.g. Galbraith, 2010; Fig. 5). Use  
357 of appropriate statistical methods for plotting and choosing an average  $D_E$  has been made simpler for  
358 the non-specialist by the recent development of the R package for Luminescence dating (Kreutzer et  
359 al., 2012). The overdispersion parameter, defined as the remaining dispersion after having considered  
360 the uncertainty sources associated with the measurement, is seen as an indicator of the likely

361 presence of partial bleaching (Colarossi et al., 2015). However, it is difficult to propose a single  
362 threshold value for this since other parameters also influence overdispersion (Thomsen et al., 2012).  
363 Following investigation of the shape of the distribution, the  $D_E$  value used for the final age  
364 determination is derived from several 'age models' (Lauer et al., 2010), all available in the R package  
365 for Luminescence (Fuchs et al., 2015). The most commonly used are the Common Age and Central  
366 Age Models (combining the calculation of overdispersion with that of the weighted mean), which are  
367 appropriate when the overdispersion is zero or low, respectively (no significant evidence for partial  
368 bleaching). The Minimum Age Model (Galbraith and Laslett, 1993) is used for samples with higher  
369 overdispersion values to identify the most well bleached aliquots and bases the age estimate on  
370 these. Finally the Finite Mixture Model (Galbraith and Green, 1990) can be applied to single grains  
371 only (Galbraith and Robert, 2012) and allows the detection of discrete populations. In all these cases,  
372 however, the choice of the age model to be used is often subjective, since there is no set threshold  
373 value of overdispersion to use for choosing between different age models. Bayesian methods have  
374 been used for a number of years by the radiocarbon community and are useful in robustly identifying  
375 outliers and thereby increasing precision. Such approaches have recently been tested on OSL  
376 samples (e.g. Cunningham and Wallinga, 2012; Guerin et al., 2015). Cunningham and Wallinga  
377 applied a combination of bootstrap likelihoods and Bayesian methods to young (<1 ka), partially  
378 bleached samples from a vertical floodplain sequence in the Netherlands. The bootstrap likelihoods  
379 were used to provide a probability density function for each sample that was statistically appropriate  
380 for Bayesian analysis. This approach was useful in this setting, but can only be applied where there is  
381 sufficient sample density for the stratigraphical relationships to be known and the age distributions to  
382 overlap.

383 The need for such complex statistical treatment of the results may be considered a drawback of the  
384 luminescence dating method, since the obtained age is dependent on the model used. However, when  
385 explained fully and justified in relation to luminescence characteristics, this approach leads to greater  
386 confidence in the robustness of the results. The selection of the "best" model then derives from a  
387 rigorous analysis of all the available data, including not only the measurement values, but also the  
388 field and sedimentological evidence (which can be useful for example to assess the bleaching  
389 potential of the sediments). Furthermore, recent developments in the use of Bayesian statistics hold  
390 out a hope that a single approach to determining equivalent dose may soon be possible where  
391 stratigraphical relationships are clear.

392 *3.5. A key issue for the future: extending OSL dating to the Middle Pleistocene*

393 Whilst fluvial sediments of Middle Pleistocene age have been dated, especially using IRSL on  
394 feldspars, extending the age range to older sediments remains a major issue (Table 3). This is also of  
395 significant importance for the FLAG community as it will allow a longer-term reconstruction of valley  
396 evolution during the Pleistocene. Several protocols have been developed to date older sediments,  
397 including the pIR-IRSL method discussed above.

398 For quartz, a new approach is the measurement of the Thermally Transferred OSL signals (TT-OSL;  
399 Wang et al., 2006). These signals are observed after stimulation and heating of the quartz grains and  
400 result from a complex charge transfer associated with the heating. As they saturate at much higher  
401 doses than the OSL signal, they might be used for dating older sediments (Table 3). Arnold et al.  
402 (2015) compared single-grain TT-OSL and pIR-IRSL at the Atapuerca hominin site where independent  
403 age control is available. When they used measurement temperatures of 225 °C, they found good  
404 agreement for both methods from ~240–930 ka, though pIR-IRSL measurements at 290 °C gave  
405 overestimates. Arnold et al. (2015) argue therefore that multiple methods should be used in extended  
406 range dating, since each is more reliable in different settings. This view seems also relevant for the  
407 new developments in Luminescence dating, such as the Infra-Red Radio-Fluorescence (IR-RF) or the  
408 Violet Simulated Luminescence, for which further investigations are required prior to validate their  
409 suitability for dating ancient fluvial archives. It is worth noting that these approaches do not address  
410 uncertainties in estimating dose rates, which remain significant also at older ages.

411 **4. Electron Spin Resonance (ESR) dating in fluvial environments**

412 ESR is a radiation exposure (or palaeodosimetric) dating method based on the evaluation of the  
413 natural radiation dose absorbed by materials over geological times. The first application of ESR as a  
414 geochronologic tool was published by Ikeya (1975) on stalagmites from Japanese caves. Since then,  
415 the method has been used on a wide range of materials including phosphates, carbonates, and  
416 silicates (see review in Ikeya, 1993). The most popular applications in fluvial context are undoubtedly  
417 on fossil teeth and optically bleached quartz grains extracted from sediment, either for targeted dating  
418 of a given site/section (e.g. Falguères et al., 2006; Santonja et al., 2014) or for the establishment of a  
419 comprehensive chronological framework for terrace staircases (e.g. Voinchet et al., 2004; Antoine et  
420 al., 2007; Cordier et al., 2012). As with Luminescence dating, ESR dating is based on the  
421 quantification of charge trapped in the crystalline lattice of a material under the effect of natural

422 radioactivity. These trapped charges give rise to an ESR signal whose intensity is proportional to the  
423 radiation dose absorbed by the sample over time. The ESR age equation is similar to that used in  
424 luminescence dating and the standard analytical procedure consists in determining the two main  
425 parameters: the equivalent dose ( $D_E$ ) and the dose rate.  $D_E$  is obtained using ESR spectroscopy, by  
426 artificially aging the samples at increasing doses in order to describe the behaviour of the studied  
427 signal. The dose rate is usually assessed by a combination of *in situ* and laboratory measurement  
428 using a wide range of different analytical techniques and corrected for the density of the material, its  
429 geometry and water content (see Grün, 1989 and Duval, 2016).

#### 430 *4.1. ESR dating of fossil teeth: on the importance of modelling uranium incorporation into dental* 431 *tissues*

432 ESR dating of fossil teeth has been first proposed in the mid-1980s as an alternative to fossil bones  
433 (see an overview by Duval, 2015 and references therein). The main difficulty of this application lies in  
434 the complexity of the system that has to be considered for the dose rate evaluation. A tooth is made  
435 from different dental tissues (dentine, enamel and, sometimes, cement). All have different  
436 characteristics in terms of composition and thickness that contribute to the irradiation of the enamel  
437 layer. Additionally, dental tissues are known to behave as open systems for U-series elements. In  
438 other words, teeth frequently experience delayed U-uptake or U-leaching processes. As a  
439 consequence, it is crucial to model the kinetics of the incorporation of U into each dental tissue in  
440 order to obtain an accurate estimation of the dose rate. The most common, and reliable, method is  
441 using the U-series data collected for each dental tissue in combination with the ESR dose evaluation  
442 (i.e., the so-called combined U-series/ESR dating approach; see Grün et al., 1988 and Grün 2009).  
443 Further detail is found in a recent review by Duval (2015) and Table 4.

#### 444 *4.2. ESR dating of sedimentary quartz grains: the choice of signal to measure*

445 Similar to OSL, ESR dating of sedimentary quartz is based on the study of light-sensitive signals  
446 whose intensity is reset (bleached) under sunlight exposure during sediment transportation. Once the  
447 sediment is buried, and thus sheltered from sunlight, paramagnetic centres are created and the ESR  
448 signal intensity increases as a result of the interaction of natural radioactivity with the quartz sample.  
449 Quartz has several paramagnetic centres associated with crystal defects (for a detailed review, see  
450 Ikeya, 1993; Preusser et al., 2009), but the most widely used since the first dating application by  
451 Yokoyama et al. (1985) are undoubtedly the Titanium (Ti) and the Aluminum (Al) centres. Because Al

452 is the major trace element found in quartz (Preusser et al., 2009), the ESR signal associated with the  
453 Al centre can be observed in any sample. It also usually presents high intensities (Fig. 6a) and signal-  
454 to-noise ratio values, ensuring high precision measurements (Duval, 2012). However, the Al signal  
455 shows relatively slow bleaching kinetics (the signal requires several hundred hours of UV laboratory  
456 irradiation to reach a minimum value, see Fig. 6b), and it cannot be fully reset under sunlight exposure  
457 as there is a residual ESR intensity that cannot be bleached (Fig. 6b; Toyoda et al, 2000). This  
458 residual level should be assessed (usually via bleaching experiments using sunlight simulators) in  
459 order to avoid dose overestimations. In contrast, the Ti centres (Ti-Li and Ti-H mostly in quartz  
460 samples) show much faster bleaching kinetics and no residual (i.e. unbleachable) ESR intensity.  
461 However, measurements are significantly longer and less precise than those of the Al centre given the  
462 very low ESR intensities that are usually measured (Fig. 6a, Duval and Guilarte, 2015). Further detail  
463 about ESR dating of optically bleached quartz grains may be found in the recent reviews by Toyoda  
464 (2015) and Tissoux (2015), while basic information is also given in Table 4.

#### 465 *4.3. Fluvial environment and ESR dating: main specificities*

466 Depending on the material dated, there may be different impacts from the fluvial environment on the  
467 ESR dating results. Unlike in quartz, the ESR signal measured in tooth enamel is not light sensitive  
468 and thus cannot be reset during transportation. However, transport and depositional conditions can  
469 indirectly impact the ESR results, in particular regarding the preservation state of the sample, as they  
470 may fragment and weaken dental tissues, thus favouring post-depositional processes and in particular  
471 U-uptake or leaching. Additionally, a review by Grün (2009) showed that the U-uptake kinetics into  
472 dental tissue is significantly different depending on the sedimentary environment: teeth found in cave  
473 sites most frequently document earlier U-uptake compared with those found in open air sites, which  
474 also show more frequent occurrences of U-leaching. This is most likely due to differences in the  
475 sedimentological context. Cave sites, as closed environments, usually offer more stable geochemical  
476 conditions over time. In contrast, open air sites are frequently found as the result of erosion processes  
477 that may induce modifications of the hydrological environment and cause recent mobilisation of  
478 radioelements impacting the original isotopic signature of the teeth.

479 Fluvial transport has a direct impact on the ESR signals measured in quartz as it is known to induce  
480 resetting by either exposure to natural sunlight (Toyoda et al., 2000) or mechanical effects (Grün and  
481 Liu, 2011). Similarly to OSL, the degree of bleaching of the ESR signals depends on the length and

482 conditions of transport (see section 3.2.). In a recent study, Voinchet et al. (2015) studied the impact of  
483 a series of parameters such as the grain size, transport mode and water turbidity to evaluate the most  
484 suitable conditions for optimum bleaching. Based on their results, higher bleaching levels were  
485 achieved for 100-200  $\mu\text{m}$  grains in comparison with other fractions and for fluvial transport under clear  
486 water conditions (see overview in Fig. 2).

#### 487 *4.4. Sampling precautions*

488 When dating sedimentary quartz, sampling precautions are very similar to those for Luminescence  
489 dating (section 3.3), i.e. the choice of a suitable sedimentary setting and suitably thick beds for  
490 simplicity of dose-rate estimation (Fig. 4). Although ESR signals bleach much slower than OSL ones, it  
491 is nevertheless important to minimise the exposure of the raw sediment to the sunlight during  
492 sampling, as in luminescence dating. According to the results shown by Voinchet et al (2015),  
493 sediment showing a non-negligible fraction of medium sands (mostly 100-200  $\mu\text{m}$ ) and transported  
494 and deposited in a clear-water fluvial environment should be targeted for sampling, as they potentially  
495 offer the most suitable bleaching conditions. In addition, *in situ* measurements of natural radioactivity  
496 should be undertaken (especially if the immediate surrounding sedimentary environment is not  
497 homogeneous, see Fig. 4b), in order to obtain an accurate estimation of the gamma dose rate.  
498 Additional small bags of sediment are also usually collected at the ESR sampling spot for future  
499 laboratory analysis, e.g. for water content evaluation and analysis of radioelement concentration.  
500 When dating teeth, samples have usually already been collected during the archaeo-palaeontological  
501 excavation and are thus chosen from collections. It is important to make sure that exact original  
502 (geographical and stratigraphical) location of the selected tooth is well-known and the corresponding  
503 layer/outcrop/site is still accessible to enable complementary fieldwork sampling and dose rate  
504 measurements. Ideally, in the case of fossil teeth it is recommended to ask the archaeologists and/or  
505 palaeontologists to collect the sediment attached to the tooth during the excavation. This is essential  
506 for a correct evaluation of the beta, and sometimes gamma, dose rate component(s). The apparent  
507 preservation state of the tooth matters as well, as previous studies have shown a strong correlation  
508 between macroscopic cracks in dental tissues and preferential migration of U-series elements (Duval  
509 et al., 2011).

#### 510 *4.5. Current challenges in ESR dating*

511 4.5.1. ESR dating of fossil tooth enamel: improving resolution and removing unstable components of  
512 the ESR signal

513 In comparison with quartz, ESR dose reconstruction of fossil tooth enamel is more straightforward.  
514 The composition of the ESR signal and its dose response has been extensively studied in recent  
515 decades. The modern development of ESR analyses of enamel fragments now enables the  
516 differentiation of the relative contribution of non-oriented  $\text{CO}_2^-$  radicals (NOCORs) vs. the oriented  
517 ones (CORs) (e.g. Grün et al., 2008). Additionally, Joannes-Boyau and Grün (2011) showed that  
518 laboratory gamma irradiation produces additional unstable NOCORs in comparison with natural  
519 irradiation, which may lead to dose underestimation (~30%) if this contribution is not removed. The  
520 authors acknowledge, however, that this value should not be considered as universal and extrapolated  
521 to any samples, as it may depend on many parameters (e.g., age, type, species). In contrast, more  
522 recent investigations indicate that this preferential creation of an unstable component may not be  
523 systematic, being rather sample dependant (Duval and Grün, unpublished data). Consequently, from  
524 these results it seems that each sample should be independently assessed. However, as an additional  
525 complication, it should be mentioned here that most of the dating studies are performed on enamel  
526 powder. One of the major current challenges would thus be to develop an analytical procedure that  
527 enables an easy identification of these unstable NOCORs using enamel powder. In that regard, using  
528 the microwave saturation characteristics of the different groups of  $\text{CO}_2^-$  (Scherbina and Brik, 2000)  
529 may be an avenue worth exploring in the future.

530 High resolution LA-ICP-MS U-series analyses has recently demonstrated the spatial heterogeneity of  
531 the distribution of U-series elements in dental tissues (Duval et al., 2011). This analytical tool has  
532 rapidly become essential for studying U-mobility and may be particularly useful to identify domains in  
533 the teeth that are suitable for ESR dating. However, the use of this technique raises new issues. There  
534 is a difference in resolution when comparing ESR and the ICP-MS methods. Currently, *in situ* laser  
535 ablation ICP-MS U-series analysis can be performed with a resolution of a few tens of  $\mu\text{m}$ . In contrast,  
536 the spatial variation of the ESR signal intensity in tooth enamel has rarely been studied, and ESR bulk  
537 analyses are usually performed on several hundreds of mg of enamel powder. This difference in  
538 resolution may become a non-negligible source of uncertainty in ESR dating, especially for old  
539 samples for which the dose rate associated with dental tissues is the major factor in the total dose rate  
540 calculation. Future challenges will thus consist of developing new approaches to reduce the amount of  
541 sample required for ESR analyses and obtain spatially resolved data. This is now possible through the

542 use of high sensitivity X-band resonators and with the development of a specific analytical procedure  
543 for quantitative measurements in Q-band spectroscopy based on only a few mg of enamel (Guilarte et  
544 al., 2016). Additionally, although it is for the moment extremely complicated to integrate spatially  
545 resolved ESR and U-series data for age calculations, the recent development of DosiVox (software for  
546 dosimetry simulations) opens new possibilities for modelling dose rates from complex geometries and  
547 heterogeneous spatial distributions of radioelements (Martin et al., 2015).

#### 548 *4.5.2. Avoiding and minimizing the effect of scatter and incomplete bleaching in ESR dating of* 549 *sedimentary quartz*

550 One of the main difficulties in ESR dating of quartz is to achieve repeatable measurements ensuring  
551 reproducible  $D_E$  results. This reproducibility is lower than that obtained with tooth enamel, not only  
552 because measurements close to liquid  $N_2$  temperature require a very stable experimental setup, but  
553 also because of the heterogeneity of the quartz samples and the strong angular dependence of the  
554 signal within the cavity. Extensive work has been performed recently to optimise the conditions of  
555 measurements for both the Al and Ti centres (e.g. Duval and Guilarte, 2012, 2015; Duval, 2012).

556 In parallel to this work, another major challenge is in reducing the uncertainty on the final  $D_E$  value. As  
557 noted by Toyoda (2015), some approaches developed in OSL dating are definitely worth exploring in  
558 ESR dating. Perhaps the most obvious is the use of the regenerative dose protocol instead of the  
559 additive dose protocol that is routinely used in ESR. This protocol would not only provide more precise  
560  $D_E$  results but also significantly shorten the analytical time (i.e. fewer aliquots to be measured and  
561 lower irradiation dose values). However, several previous attempts employing optical bleaching  
562 resetting have shown somewhat contrasting results regarding the presence of sensitivity changes  
563 (Tissoux et al., 2007; Beerten and Stesmans, 2006). Other approaches are less obviously fruitful. For  
564 example, although single grain dating using Q-band ESR spectroscopy has been tested to identify  
565 partial bleaching among a grain population, it is currently too complicated to be applied routinely  
566 (Beerten and Stesman, 2006).

567 The main challenge, however, is in minimising the uncertainty regarding possible incomplete  
568 bleaching of the signal during sediment transportation. Most dating studies use the Al centre even  
569 though laboratory bleaching experiments indicate that several hundreds of hours of exposure to UV  
570 are required for the ESR signal to decay to a plateau (e.g. Toyoda et al., 2000; see also Fig. 6b).  
571 These values would correspond to several tens of days of sunlight, which understandably leads many

572 authors to question the possibility of the Al centre actually reaching its residual ESR intensity during  
573 transportation. However, Voinchet et al. (2007) demonstrated that the signal was fully reset (to its  
574 residual level) after only 1 km of transportation in the Creuse river, France. Additionally, at the  
575 Vallparadís site (Spain), Al-ESR ages were found to be in good agreement with the US-ESR ages on  
576 fossil teeth and data from magneto- and bio-stratigraphy (Duval et al., 2015). These two examples  
577 demonstrate that any definitive conclusion derived from laboratory bleaching experiments should be  
578 considered with caution. It is possible that other processes, not yet understood, are involved in the  
579 bleaching of the signal in natural conditions.

580 As a consequence of the uncertainty that may arise from the bleaching of the Al centre, ESR age  
581 results based on this centre should be considered as maximum possible ages: the true age of the  
582 deposits being either similar or younger. To constrain this uncertainty, a few strategies are available.  
583 The use of modern analogue samples collected from nearby river banks may provide some useful  
584 information regarding resetting of the signal. This approach is, however, based on the assumption that  
585 transportation and bleaching conditions are similar to those in the past, which is not always plausible.  
586 Another approach is to use independent age control to verify the age results (see the example of  
587 Vallparadís, Duval et al., 2015). However, the best option is undoubtedly the Multiple Centres (MC)  
588 approach proposed by Toyoda et al (2000). The authors proposed the systematic measurement of  
589 both the Ti-Li and Al centres in quartz samples in order to check whether they would provide  
590 consistent results (Table 5). If the Al centre yields an age estimate older than that of the Ti centre, this  
591 is interpreted as incomplete bleaching of the Al signal. In this case, the Ti-Li age should be considered  
592 a closer estimate to the burial age of the deposits. Although ESR measurements following the MC  
593 approach are highly time consuming, it has provided promising results (see Rink et al., 2007; Duval et  
594 al., 2015). The use of this MC may soon become a standard requirement in ESR dating of optically  
595 bleached quartz grains.

596 Lastly, another Ti centre, Ti-H, presents great potential worth investigating for dating purposes. It is  
597 known to bleach much faster and to be more radiosensitive than the Ti-Li (see Fig. 6b; Duval and  
598 Guilarte, 2015), which would make it a good candidate for dating deposits younger than 200 ka. It is,  
599 however, unclear for the moment whether it provides reliable dose estimations. Indeed, the weakness  
600 of the signal intensity makes it very complicated to measure in all samples, resulting in low  
601 measurement precision (Table 5; Duval and Guilarte, 2015).

## 602 5. $^{230}\text{Th}/\text{U}$ -dating of fluvial deposits

603 The  $^{230}\text{Th}/\text{U}$ -dating method is based on the radioactive decay in the natural decay chain of  $^{238}\text{U}$  and  
604 was developed in the 1960s (Broecker, 1963; Kaufman and Broecker, 1965). Since then, the precision  
605 and accuracy of the method has progressively increased, primarily due to major technical advances.  
606 Whereas alpha spectrometry was widely used until the 1990s (Goldstein and Stirling, 2003), the use of  
607 thermal ionisation mass spectrometry (TIMS) (Edwards et al., 1987) represented a major advance at  
608 the end of the 1980s. This reduced the time required for an analysis from a week to several hours,  
609 decreased sample size from 10-100 g to 0.1-1 g and, most importantly, improved precision from  
610 percent to permil levels and extending the dating range from 350 to 600 ka (Goldstein and Stirling,  
611 2003). In the last two decades, the application of multi-collector inductively coupled plasma mass  
612 spectrometry (MC-ICPMS) has led to further substantial improvements (Goldstein and Stirling, 2003;  
613 Scholz and Hoffmann, 2008). The considerably higher ionisation and transfer efficiency for U and Th  
614 isotopes of the MC-ICPMS technique leads to higher count rates, in turn resulting in more precise and  
615 accurate  $^{230}\text{Th}/\text{U}$ -ages. Furthermore, measurement times (~10-20 minutes) and sample sizes are  
616 again substantially lower than for TIMS. In addition to the technical advances, the half-lives of both  
617  $^{230}\text{Th}$  and  $^{234}\text{U}$  have been re-determined (Cheng et al., 2000, 2013), also leading to more precise  
618  $^{230}\text{Th}/\text{U}$ -ages. During the last decade, procedures for laser-ablation (LA) MC-ICPMS  $^{230}\text{Th}/\text{U}$ -dating of  
619 carbonates have been developed (e.g. Eggins et al., 2005; Mertz-Kraus et al., 2010). This technique  
620 has very large potential since it offers *in situ* dating at extremely high spatial resolution (in the range of  
621 10-100  $\mu\text{m}$ ), requires no sample preparation and is extremely fast and, thus, enables very high sample  
622 throughput. In return, the analytical precision is much lower than for conventional  $^{230}\text{Th}/\text{U}$ -ages (a few  
623 percent compared to epsilon levels).

624 In undisturbed natural materials with an age of several million years, the activity of the parent (i.e.  
625  $^{238}\text{U}$ ) and the daughter isotopes (i.e.  $^{234}\text{U}$  and  $^{230}\text{Th}$ , respectively) is in secular equilibrium. This state of  
626 equilibrium, however, can be disturbed by several natural processes, which is the basic principle of all  
627 U-series disequilibrium dating methods. In aqueous environments, the major reason for disequilibrium  
628 between U and Th is the different geochemical behaviour of the two elements. Whereas U is soluble,  
629 Th is insoluble in natural waters and, thus, mainly transported adsorbed onto particles. As a  
630 consequence, groundwater, rivers, lakes and seawater contain significant amounts of dissolved U, but  
631 essentially no Th. During formation of secondary carbonates, U is thus incorporated, whereas Th is  
632 not. Consequently, secular equilibrium is disturbed, and the initial activity of  $^{230}\text{Th}$  is zero. If the decay

633 system remains closed after deposition (i.e. no U and Th isotopes are lost or added subsequently), the  
634 activity ratios of ( $^{234}\text{U}/^{238}\text{U}$ ) and ( $^{230}\text{Th}/^{238}\text{U}$ ) return to the state of secular equilibrium (e.g. Bourdon et  
635 al., 2003, activity ratios are indicated in parentheses in the following). The temporal evolution of the  
636 activity ratios (in particular the increase of  $^{230}\text{Th}$  due to the decay of  $^{234}\text{U}$  and  $^{238}\text{U}$ ) allows dating of the  
637 time of carbonate formation (i.e. the timing of the establishment of disequilibrium) and, thus, the age of  
638 the carbonate phase. This is, however, only possible if two basic requirements are fulfilled: (i) no  
639 presence of initial  $^{230}\text{Th}$  and (ii) the system remained closed after deposition. If one of these  
640 assumptions is violated, the resulting  $^{230}\text{Th}/\text{U}$ -age may be substantially inaccurate.

641  $^{230}\text{Th}/\text{U}$ -dating can, in principle, be applied to all materials whose formation is accompanied by a  
642 constrained disequilibrium between U and Th. The materials most widely dated by the  $^{230}\text{Th}/\text{U}$ -method  
643 are fossil reef corals and speleothems (Scholz and Hoffmann, 2008; Edwards et al., 2003), which can,  
644 in general, be accurately and precisely dated up to an age of 600 ka. However, with increasing  
645 sensitivity of both LA and MC-ICPMS systems, increasing precision may be achieved enabling high-  
646 precision *in situ*  $^{230}\text{Th}/\text{U}$ -dating (i.e., without prior sample preparation) at very high spatial resolution.  
647 This may be particularly useful for impure carbonates found in fluvial deposits in order to analyse the  
648 most pristine fractions of a dirty sample. Examples of successful dating of inclusions in fluvial deposits  
649 by the  $^{230}\text{Th}/\text{U}$ -method (Fig. 2) include pedogenic carbonates and calcretes deposited in alluvial fans  
650 and river terraces (e.g. Candy et al., 2004; Kelly et al., 2000; Ludwig and Paces, 2002; Sharp et al.,  
651 2003) as well as tufa and travertine (Schulte et al., 2008; Candy and Schreve, 2007). All these  
652 deposits have in common that they form subsequently to the deposition of fluvial sediments, such as  
653 fans and terraces (Fig. 2). Thus, they can only provide a minimum age for the fluvial deposits with  
654 which they are associated (Blisniuk et al., 2012). Carbonates that have been mobilised subsequent to  
655 deposition (e.g. flood events or washed in from slopes, Fig. 2) are not expected to provide reliable  
656  $^{230}\text{Th}/\text{U}$ -ages because they are (i) most likely affected by post-depositional diagenesis and (ii) difficult  
657 to relate to a depositional context (Fig. 2). Extensive reviews of the  $^{230}\text{Th}/\text{U}$ -dating methodology can be  
658 found in the classic books by Ivanovich and Harmon (1992) and Bourdon et al. (2003).

#### 659 5.1. $^{230}\text{Th}/\text{U}$ -dating of secondary carbonates in fluvial archives: main issues

660 In general, carbonates deposited in fluvial and lacustrine environments are difficult to date by the  
661  $^{230}\text{Th}/\text{U}$ -method. In many cases, samples of fluvial and lacustrine deposits contain very large amounts  
662 of detrital Th, which represents a violation of one of the basic requirements of the dating method.

663 Since Th is mainly transported adsorbed onto particles, it is generally associated with relatively fast  
664 flowing water, which has the potential to transport these particles. In particular, carbonates associated  
665 with alluvial fans thus often contain substantial amounts of detrital Th (Fig. 2). However, pedogenic  
666 carbonates may also contain high amounts of detrital Th, which is mobilised from the overlying  
667 horizons (Fig. 2). These materials are thus often referred to as impure carbonates or dirty calcites  
668 (e.g., Kaufman, 1993). Initial Th is often associated with a silicate or clay fraction. Whereas the  
669 preparation of pure carbonate samples is relatively straightforward (e.g. Yang et al., 2015), the  
670 preparation of impure carbonates may be more elaborate due to the presence of an insoluble residue.  
671 Various approaches to deal with insoluble residues have been proposed (see section 5.2.2). Initial  
672 (also often referred to as *detrital*)  $^{230}\text{Th}$  is generally accompanied by  $^{232}\text{Th}$ , which is the most abundant  
673 naturally occurring isotope of Th.  $^{232}\text{Th}$  does not occur in the decay chain of  $^{238}\text{U}$  and is, in contrast to  
674  $^{230}\text{Th}$ , not produced by the decay of  $^{234}\text{U}$  and  $^{238}\text{U}$ . Elevated content of  $^{232}\text{Th}$  is clear evidence for the  
675 presence of initial  $^{230}\text{Th}$ , and its concentration even provides a measure for the degree of  
676 contamination. For ( $^{230}\text{Th}/^{232}\text{Th}$ ) activity ratios  $<20$ , a correction for detrital contamination is definitely  
677 required (Schwarcz, 1989). Other studies have suggested even higher thresholds for ( $^{230}\text{Th}/^{232}\text{Th}$ )  
678 necessitating a correction for detrital contamination (Richards and Dorale, 2003). Potential correction  
679 techniques that have been shown to be successful for fluvial deposits are discussed in sections 5.2.1.  
680 and 5.2.2. In addition, post-depositional open-system behaviour is not uncommon for secondary  
681 carbonates deposited in fluvial environments, which is even more complicated to detect and account  
682 for (see 5.2.3.). For marine samples, such as corals, open system behaviour can be detected by  
683 comparing the initial ( $^{234}\text{U}/^{238}\text{U}$ ) activity ratio of the sample with the ( $^{234}\text{U}/^{238}\text{U}$ ) activity ratio of modern  
684 seawater (e.g. Edwards et al., 2003). In terrestrial environments, this is not possible due to the highly  
685 variable ( $^{234}\text{U}/^{238}\text{U}$ ) activity ratio in river, lake and groundwater. Thus, successful  $^{230}\text{Th}/\text{U}$ -dating of  
686 fluvial carbonates has been restricted to a relatively small number of case studies, which are  
687 characterised by the high U content ( $^{238}\text{U}>1\ \mu\text{g/g}$ ) of the dated material.

## 688 5.2. Approaches developed to date secondary carbonates by $^{230}\text{Th}/\text{U}$

689 Two general correction methods to account for detrital Th have been developed: *a priori* estimation of  
690 the ( $^{230}\text{Th}/^{232}\text{Th}$ ) activity ratio of the detrital phase and isochron techniques. In rare cases, secondary  
691 carbonates associated with fluvial deposits, such as tufa and travertine, may be very clean, and a  
692 correction for initial  $^{230}\text{Th}$  may not be necessary. For instance, Schulte et al. (2008) established a  
693 chronology for the fluvial terrace sequence from the River Aguas basin, Iberian Peninsula, by  $^{230}\text{Th}/\text{U}$ -

694 dating of travertine. The ( $^{230}\text{Th}/^{232}\text{Th}$ ) activity of some of their samples is larger than 20, and a  
695 correction for initial  $^{230}\text{Th}$  is not required. Candy and Schreve (2007) obtained  $^{230}\text{Th}/\text{U}$ -ages on fluvial  
696 and colluvial tufa deposits from southern England with sufficient precision to correlate discrete periods  
697 of temperate climate with individual warm sub-stages during MIS 7. Although the U content of their  
698 samples is relatively low (ca. 0.1  $\mu\text{g/g}$ ), the ( $^{230}\text{Th}/^{232}\text{Th}$ ) activity of the majority of samples is  $>20$ .

#### 699 5.2.1. *A priori estimation of the ( $^{230}\text{Th}/^{232}\text{Th}$ ) activity ratio of the detrital phase*

700 The average  $^{232}\text{Th}/^{238}\text{U}$  weight ratio of the upper continental crust is  $\sim 3.8$  (Wedepohl, 1995). Assuming  
701 secular equilibrium between  $^{230}\text{Th}$ ,  $^{234}\text{U}$  and  $^{238}\text{U}$  for the detrital component, the ( $^{230}\text{Th}/^{232}\text{Th}$ ) activity  
702 ratio of the initial Th is  $\sim 0.9$  (Hellstrom, 2006). Based on the measured content of  $^{232}\text{Th}$ , the amount of  
703 initial (detrital)  $^{230}\text{Th}$  can thus be estimated and subtracted from the measured concentration of  $^{230}\text{Th}$ .  
704 This approach is often referred to as a *a priori* estimation of the detrital phase and may provide  
705 reasonable ages. However, the initial ( $^{230}\text{Th}/^{232}\text{Th}$ ) activity ratio is highly variable and associated with  
706 large uncertainties. Usually, an uncertainty of 50% is assumed (Hellstrom, 2006). Propagation of this  
707 substantial uncertainty to the corrected  $^{230}\text{Th}/\text{U}$ -age may lead to highly elevated age uncertainties and  
708 even ages with zero significance (Kaufman, 1993; Wenz et al., 2016). Despite these large  
709 uncertainties, a *a priori* estimation of the ( $^{230}\text{Th}/^{232}\text{Th}$ ) activity ratio of the detrital phase has been  
710 successfully applied to date fluvial deposits by the  $^{230}\text{Th}/\text{U}$ -method. For instance, Adamson et al.  
711 (2014) obtained a large number of ages for fluvial deposits in Montenegro by  $^{230}\text{Th}/\text{U}$ -dating of  
712 carbonate benches and calcite rinds. This study is particularly remarkable because the U content of  
713 the studied samples was relatively low ( $<1 \mu\text{g/g}$ ). However, many samples also have very low  $^{232}\text{Th}$ ,  
714 resulting in ( $^{230}\text{Th}/^{232}\text{Th}$ ) activity ratios  $>20$ . Ludwig and Paces (2002) determined  $^{230}\text{Th}/\text{U}$ -ages on  
715 pedogenic silica-carbonate clast rinds and matrix laminae from alluvium in Crater Flat, Nevada,  
716 employing the TSD-technique, whereas Sharp et al. (2003) dated pedogenic carbonate clast-rinds  
717 from gravels of glacio-fluvial terraces in the Wind River Basin, Wyoming. The success of both studies  
718 is mainly based on the high U content of the samples. Blisniuk and Sharp (2003) determined the age  
719 of two well-preserved fluvial terrace surfaces in central Tibet by  $^{230}\text{Th}/\text{U}$ -dating of pedogenic carbonate  
720 rinds on clasts in the terrace deposits.

#### 721 5.2.2. *Isochron methods*

722 The second approach to account for initial or detrital  $^{230}\text{Th}$  is the isochron methodology. For isochron  
723  $^{230}\text{Th}/\text{U}$ -dating of impure carbonates, various procedures for sample preparation have been proposed

724 (e.g. total sample dissolution (TSD), leachate-leachate (L/L), leachate-residue (L/R), Bischoff and  
725 Fitzpatrick, 1991; Kaufman, 1993; Ku and Liang, 1984; Luo and Ku, 1991; Schwarcz and Latham,  
726 1989). In addition, several statistical methods for the evaluation of the isochron data have been  
727 developed (Ludwig, 2003). In general, the isochron method is more flexible than the *a priori* approach  
728 and provides more reliable ages with smaller uncertainties (Wenz et al., 2016). However, the  
729 application of the isochron methodology is based on two assumptions: all sub-samples (i) must have  
730 the same age and (ii) should contain different amounts of the same detrital component (i.e. with the  
731 same ( $^{234}\text{U}/^{238}\text{U}$ ) and ( $^{230}\text{Th}/^{238}\text{U}$ ) ratios). Unfortunately, the latter assumption in particular is not  
732 fulfilled for many impure carbonate samples (Ludwig, 2003; Wenz et al., 2016), again leading to large  
733 age uncertainties and corrected ages with low significance. Isochron techniques have also been  
734 successfully applied for  $^{230}\text{Th}/\text{U}$ -dating of fluvial deposits. For instance, a stratigraphically consistent  
735 chronology based on isochron  $^{230}\text{Th}/\text{U}$ -ages determined on pedogenic calcretes has been reported for  
736 alluvial terrace sequences from the Sorbas Basin, south-eastern Spain (Candy et al., 2004, 2005;  
737 Kelly et al., 2000). However, Candy et al. (2005) have shown that dating of mature calcretes is much  
738 more difficult than dating of immature calcretes, as has been revealed by the isochron statistics.  
739 Nevertheless, it may also be possible to determine a reliable age for mature calcretes if a large  
740 number of sub-samples from a single horizon are dated. Other studies aiming to date fluvial deposits  
741 were not successful in accounting for initial  $^{230}\text{Th}$  by isochron techniques. For instance, Kock et al.  
742 (2009) attempted  $^{230}\text{Th}/\text{U}$ -dating of pedogenic carbonate crusts from fluvial gravels of the River Rhine,  
743 and compared them with internally coherent OSL ages. Most of their U-series data scattered widely on  
744 isochron diagrams suggesting multiple components of initial  $^{230}\text{Th}$  that are not related to detrital  $^{232}\text{Th}$ .  
745 A significant fraction of the initial  $^{230}\text{Th}$  may originate from bacterial activity and Th transport on organic  
746 colloids. This suggests that samples in which bacteria could have contributed to carbonate  
747 precipitation should be avoided.

### 748 5.2.3. Accounting for open-system behaviour

749 One option for detecting open-system behaviour of  $^{230}\text{Th}/\text{U}$ -ages of fluvial deposits is through  
750 comparison with independent ages (e.g. Blisniuk et al., 2012; see section 7). Another option is  
751 consideration of the stratigraphical context of the deposited samples, i.e. whether the determined  
752 (corrected)  $^{230}\text{Th}/\text{U}$ -ages are in stratigraphical order within a sedimentary sequence. This approach is  
753 currently used to identify ages representing outliers, probably because the applied correction  
754 techniques were not successful or due to post-depositional open-system behaviour. This approach

755 has been proved to be successful for the aragonitic lacustrine sediments from Lake Lisan, the Last  
756 Glacial precursor of the Dead Sea, which have been extensively studied by  $^{230}\text{Th}/\text{U}$ -dating (e.g.,  
757 Torfstein et al., 2013). These sediments contain high amounts of U ( $>3\ \mu\text{g/g}$ ), and different  
758 approaches have been used to obtain corrected ages, including isochrons (Schramm et al., 2000), a  
759 *priori* estimates of the detrital ( $^{230}\text{Th}/^{232}\text{Th}$ ) activity ratio (Schramm et al., 2000) and an iterative  
760 approach independently evaluating the composition of the detrital component for every set of coeval  
761 samples (Torfstein et al., 2013). Furthermore, several authors recently have suggested algorithms for  
762 speleothems including stratigraphical constraints in order to estimate the ( $^{230}\text{Th}/^{232}\text{Th}$ ) activity ratio of  
763 the detrital component (Hellstrom, 2006; Roy-Barman and Pons-Branchu, 2016). These algorithms  
764 may also be very useful for fluvial samples deposited in a clear stratigraphical context.

## 765 **6. Terrestrial cosmogenic nuclides (TCN) dating of fluvial deposits**

766 The development of the AMS technology in the early 1980s (e.g. Klein et al., 1982), which allowed  
767 measurements of isotopic ratios as low as  $10^{-15}$  at that time (presently  $10^{-16}$  has been reached),  
768 represented a decisive milestone, enabling the use of TCN as a dating tool, as proposed by Davis and  
769 Schaeffer (1955). In parallel, a tremendous amount of work has taken place and aimed at  
770 understanding the physical properties and processes involved in the production of the most commonly  
771 used nuclides in the Earth sciences, i.e.  $^3\text{He}$ ,  $^{10}\text{Be}$ ,  $^{21}\text{Ne}$ ,  $^{26}\text{Al}$  and  $^{36}\text{Cl}$  (e.g. Nishiizumi et al., 1986; see  
772 reviews of Gosse and Phillips, 2001; Dunai, 2010). A particular emphasis was on the determination  
773 and refinement of their respective production rates according to the different production pathways,  
774 mostly involving fast neutron- (spallation) and muon-induced reactions (Gosse and Phillips, 2001). This  
775 is well exemplified by the strongly debated determination of both the production rate of  $^{10}\text{Be}$  in quartz  
776 and the half-life of this radionuclide (Gosse and Phillips, 2001; Dunai, 2010). Moreover, the use of  
777 these nuclides as geochronometers required integrating the variability of production rates in space and  
778 time, hence the build-up of scaling factors (Dunai, 2010).

779 Depending on the aim of the study and/or the fluvial or lacustrine environment where it takes place,  
780 numerical ages based on concentration measurements of cosmogenic nuclides can be undertaken  
781 either via surface exposure dating or burial dating (Fig. 2). Both dating approaches are presented in  
782 this section. Note that the material that has to be dated undergoes pre-exposure to cosmic rays during  
783 (i) bedrock exhumation, (ii) temporary storage on hillslopes and (iii) transport and/or temporary storage  
784 in the fluvial system (Fig. 2). This accumulation of cosmogenic nuclides inventories prior to the

785 depositional event is known as inheritance (Anderson et al., 1996). Whereas surface exposure dating  
786 of depositional landforms is highly sensitive to this process (see 6.1), this inherited component allows  
787 the dating of a burial event (see 6.2). In fluvial settings, surface exposure dating first provided  
788 numerical ages for alluvial fans (Siame et al., 1997; Van der Woerd et al., 1998) and river terraces,  
789 both bedrock strath terraces (Burbank et al., 1996; Leland et al., 1998) and alluvium-mantled terraces  
790 (Anderson et al., 1996, Repka et al., 1997). In lacustrine environments, surface exposure dating of  
791 palaeo-shorelines provides information about former lake-level highstands (Rades et al., 2013). Burial  
792 dating can be applied to in cave-deposited alluvium (Granger et al., 1997) or deeply buried fluvial or  
793 lacustrine sediments (Kong et al., 2009).

#### 794 *6.1. Surface exposure dating*

795 The calculation of exposure ages requires both high-precision AMS measurements of nuclide  
796 concentrations and the determination of the site-specific nuclide production rate. The latter must  
797 integrate the use of specific scaling factors and the potential topographic or self shielding of cosmic  
798 rays at the sampling location (Dunai, 2010). As fluvial sediments or related landforms very often  
799 contain quartz-bearing material, surface exposure ages are usually determined via concentration  
800 measurements of  $^{10}\text{Be}$  (Fig. 7a, Dunai, 2010), sometimes used alongside  $^{26}\text{Al}$  (e.g. Repka et al., 1997;  
801 Rixhon et al., 2011). However, alternative nuclide species are produced in other minerals, such as  $^3\text{He}$   
802 in olivine and pyroxene or  $^{36}\text{Cl}$  in calcite (see Gosse & Phillips, 2001; Dunai, 2010), thereby allowing  
803 other lithologies to be dated (e.g. Baynes et al., 2015). The dateable range in surface exposure dating  
804 of fluvial environments varies strongly according to the setting and the employed nuclide(s) (Fig. 1).  
805 The lower age range very much depends on the detection limit of the AMS, hence the production  
806 rates, but late Holocene exposure ages of bedrock strath surfaces were obtained (Leland et al., 1998,  
807 see 6.1.2.). On the other hand, surface exposure dating with  $^{10}\text{Be}$ , because of its long half-life (i.e.  
808  $\sim 1.36$  Ma), permits pre-Quaternary applications under specific conditions without saturation being  
809 reached (Dunai, 2010).

810 In many instances, surface exposure ages of fluvial depositional surfaces, especially alluvial fans,  
811 were formerly based on concentration data obtained from individual clasts or boulders lying on these  
812 (Fig. 7a, b; e.g. Siame et al., 1997; Van der Woerd et al., 1998). However, Schmidt et al. (2011)  
813 emphasized the need of caution when inferring exposure ages from such TCN concentration data;  
814 diverse geomorphological processes acting on a surface might indeed represent a considerable

815 source of uncertainty. These encompass inheritance (Fig. 2), post-depositional weathering, erosion or  
816 covering by sediments and even by snow (e.g. Anderson et al., 1996; Rixhon et al., 2011). Whereas  
817 inheritance might lead to an overestimate of the true exposure age, all other processes tend to reduce  
818 the cosmogenic inventory near the dated surfaces and thereby result in age underestimations. An  
819 unequal distribution and/or intensity of these stochastic processes across the surface might result in a  
820 significant spread in apparent exposure ages (Owen et al., 2014). For this reason thorough field  
821 observations and descriptions are an absolute prerequisite for surface exposure sampling (see field  
822 template in Dunai, 2010).

### 823 *6.1.1. Depth profile dating of depositional surfaces (alluvial fans, alluvium-mantled terraces)*

824 The depth profile sampling technique may overcome some of the uncertainties related to these  
825 geomorphological processes (Anderson et al., 1996). It allows simultaneous computation of exposure  
826 time (i.e. the abandonment time of the landform), the post-depositional denudation rate of the landform  
827 and inheritance (Braucher et al., 2009; Hidy et al., 2010). This approach consists of sampling the  
828 fluvial sediments at regular depth intervals (Fig. 7c), taking advantage of the spallation-dominated  
829 production at or near the surface and the muon-dominated production at greater depth (Braucher et  
830 al., 2009). Given the physical properties of these particles, an exponential decrease of TCN  
831 concentrations along the depth profile is expected and can be modelled by Monte Carlo simulations  
832 (Fig. 7d, see the user-friendly simulator of Hidy et al., 2010). However, because this method is very  
833 sensitive to any post-depositional reworking processes (e.g. cryo- or bioturbation...), one should avoid  
834 sites where such processes have occurred.

835 The depth profile technique is particularly useful for dating alluvial fans and fill terraces (Fig. 7d, e.g.  
836 Repka et al., 1997; Le Dortz et al., 2011; Rixhon et al., 2011). In contrast to the pioneering studies on  
837 alluvial fans (e.g. Siame et al., 1997), almost all recent works systematically combined surface  
838 concentration data with depth profile data to better constrain the inheritance and the post-depositional  
839 evolution of the landform (e.g. Le Dortz et al., 2011; Schmidt et al., 2011; Owen et al., 2014). Where  
840 the petrographic composition of fan - or terrace - sediments is favourable, it is advisable to perform an  
841 internal control by comparing concentrations of different nuclides. For instance, quartz-bearing and  
842 calcite-bearing materials enable  $^{10}\text{Be}$  and  $^{36}\text{Cl}$  concentration measurements, respectively (Le Dortz et  
843 al., 2011). As lateral or vertical offsets disrupting fan surfaces represent an excellent  
844 geomorphological marker for crustal deformation, surface exposure ages allow quantifying average

845 slip rates along main fault lines for the Middle/Late Pleistocene and/or the Holocene (e.g. Siame et al.,  
846 1997; Le Dortz et al., 2011). Also, surface exposure dating of fan surfaces may likewise provide  
847 valuable information about climatic forcing on fan formation (e.g. Owen et al., 2014). Depth profile  
848 concentration data of terrace sediments are commonly used to quantify incision rates by sampling  
849 vertically-spaced levels within terrace sequences (e.g. Repka et al., 1997). Alternatively, diachronic  
850 abandonment times of geometrically-correlated terraces along a hydrological network allow inference  
851 of long-term propagation rates of a specific incision wave from the main trunk into its (sub-)tributaries  
852 (Rixhon et al., 2011).

### 853 *6.1.2. Surface exposure dating of strath terraces*

854 An alternative application of the surface exposure method consists of dating bedrock surfaces of strath  
855 terraces (Fig. 2). This term is used here to describe laterally-carved benches in steep valley flanks,  
856 especially in actively uplifting orogens (e.g. Himalayas), and are often characterized by smooth  
857 polished surfaces or sculpted erosional features (Fig. 7e, Burbank et al., 1996; Leland et al., 1998).  
858 Inheritance usually does not represent a major issue for strath terraces since they are erosional  
859 landforms. Provided that the bedrock surface is still pristine, one can assume insignificant weathering  
860 or erosion after strath abandonment. If the strath was not covered by temporary alluvium or landslide  
861 deposits subsequent to terrace abandonment (see Leland et al., 1998), the calculation of the exposure  
862 time is straightforward (Fig. 7f, g). To check the representativeness of bedrock samples and to take  
863 concentration variability into account, we recommend the nested sampling strategy of Reusser et al.  
864 (2006). The thin alluvial cover can also be sampled if it is present (e.g. Reusser et al., 2006). Surface  
865 exposure dating of strath terraces in diverse gorge settings highlighted, for instance, (i) differential  
866 rock uplift related to major thrust activity in active orogens (Burbank et al., 1996; Leland et al., 1998),  
867 (ii) regional, climatically-driven incision of rivers along a passive margin (Fig. 7f, g, Reusser et al.,  
868 2006) or (iii) the impact of extreme flood events for canyon formation related to significant knickpoint  
869 retreat (Baynes et al., 2015).

### 870 *6.2 Burial dating*

871 In contrast to surface exposure dating, which relies on continuous accumulation of TCN, burial dating  
872 is based on the differential decay of at least two nuclides, where at least one of them is a radionuclide  
873 – for full details, see Granger and Muzikar (2001) and Granger (2014). The nuclide pair  $^{26}\text{Al}/^{10}\text{Be}$  is  
874 frequently employed because they are both produced in quartz and their production ratio is

875 fundamentally independent from latitude and altitude and varies only slightly with depth (Dunai, 2010;  
876 Granger, 2014). In the case of the pair  $^{26}\text{Al}$  and  $^{10}\text{Be}$ , burial dating is based on a two step  
877 exposure/shielding episode of any quartz-bearing material. First, the latter accumulates nuclide  
878 inventories during exhumation of bedrock and transport/storage on hillslopes and in the drainage  
879 network (Fig. 2), i.e. the inherited component. Whilst the amount of both nuclides in any given clast or  
880 grain is impossible to predict due to stochastic individual exposure history,  $^{10}\text{Be}$  and  $^{26}\text{Al}$   
881 concentrations are related as they are produced in the same material over the same time period,  
882 resulting in a  $^{26}\text{Al}/^{10}\text{Be}$  surface concentration ratio of  $\sim 6.75:1$  (Dunai, 2010; Granger, 2014). Second,  
883 the quartz-bearing material is rapidly buried (see section 6.2.1.), implying a cessation of production  
884 (Fig. 2). Exploiting the differential radioactive decays of both nuclides, the preburial ratio decreases  
885 with increasing burial duration according to the corresponding half-lives of each nuclide (Dunai, 2010).  
886 The time range of application of burial dating extends into the Pliocene ( $\sim$ up to 5 Ma; Fig. 1) but the  
887 current analytical precision of  $^{26}\text{Al}$  measurements in AMS implies uncertainties of (at least)  $\sim 60$  to 100  
888 ka (Dunai, 2010; Granger, 2014).

#### 889 *6.2.1. Complete and fast burial: dating of in cave-deposited alluvium*

890 Fast and complete burial of sediments requires two basic assumptions (Granger and Muzikar, 2001).  
891 First, the time span over which incomplete shielding occurs is much shorter than the subsequent burial  
892 duration. Second, shielded sediments are buried sufficiently deeply, i.e. in practice  $\geq 30$  m, implying an  
893 insignificant production through muons at depth. Given that these prerequisites are frequently met for  
894 in-cave deposited alluvium (Fig. 2), the sampling of these sediments is one of the most straightforward  
895 applications of burial dating (Dunai, 2010). River sediments washed into abandoned phreatic tubes in  
896 limestone valley walls characterize the last time the passage was at the local water table (Fig. 8a,  
897 Anthony and Granger, 2007). Alluvium-filled multi-level cave systems thus mimic alluvium-mantled  
898 terrace staircases and, as such, also record the regional incision history of river systems (Fig. 8b,  
899 Anthony and Granger, 2007). The selection of suitable sampling sites should ensure that abandoned  
900 and alluvium-filled phreatic tubes were not contaminated by any reworked material from an older (or  
901 younger) depositional episode (Dunai, 2010). The solution of the complete and fast burial dating  
902 equations is graphically expressed on the so-called erosion-burial diagram, where the  $^{26}\text{Al}/^{10}\text{Be}$  ratio is  
903 plotted against  $^{10}\text{Be}$  concentrations (Fig. 8c). This approach has provided valuable new insights into  
904 long-term incision rates in diverse tectonically-active (Fig. 8b, e.g. Stock et al., 2004) and moderately-

905 uplifted (e.g. Granger et al., 1997; Anthony and Ganger, 2007) settings, or in river catchments marked  
906 by enhanced glacial deepening (Häuselmann et al., 2007).

### 907 6.2.2. *Overcoming incomplete shielding: isochron burial dating of fill terraces*

908 The  $\geq 30$  m overburden thickness as a prerequisite for a complete shielding is unfortunately not often  
909 met in cases of river terraces, even in thick fill terraces (Fig. 8d). In these instances, incomplete  
910 shielding of the fluvial sediment to the cosmic rays may imply significant postburial production through  
911 deeply-penetrating muons (Granger and Muzikar, 2001). As postburial production is very difficult to  
912 constrain, it may become a considerable issue to produce reliable burial ages. This problem was  
913 overcome by the isochron burial dating method (Balco and Rovey, 2008), which involves the sampling  
914 of several pebbles from the same stratigraphical layer at the base of the river terrace (Erlanger et al.,  
915 2012; Darling et al., 2013). It relies on the fact that these clasts are likely to have originated from  
916 different source areas in the catchment (Erlanger et al., 2012). As the latter is subject to variable  
917 production and/or surface erosion rates, and clasts have variable transport and/or storage time within  
918 the fluvial system, they have distinct pre-burial histories resulting in different  $^{10}\text{Be}$  and  $^{26}\text{Al}$  inherited  
919 concentrations. Sampling the same stratigraphical layer implies an identical postburial production for  
920 each of them; this parameter can thus be treated as a constant among samples (Erlanger et al.,  
921 2012). On the graphical representation of isochron burial dating ( $^{26}\text{Al}$  concentration plotted against  
922  $^{10}\text{Be}$  concentration), the burial age is calculated from the slope of the regression line (Fig. 8e). Used  
923 on a well-preserved terrace flight in South Africa (Sundays River), this approach yielded valuable  
924 terrace ages for inferring Late Cenozoic incision rates (Erlanger et al., 2012).

### 925 6.3. *Future potential of TCN dating*

926 In addition to the commonly employed TCN ( $^3\text{He}$ ,  $^{10}\text{Be}$ ,  $^{21}\text{Ne}$ ,  $^{26}\text{Al}$  and  $^{36}\text{Cl}$ ), the use of further  
927 radionuclides may extend the application time span of TCN. On the one hand, the long-lived  $^{53}\text{Mn}$   
928 nuclide, given its half-life of  $3.7 \pm 0.4$  Ma, has the potential to unravel exposure histories older than 10  
929 Ma in iron-bearing materials, although it requires AMS technologies with higher energies than those  
930 presently attained in order to reduce the analytical uncertainty (Schäfer et al., 2006). On the other  
931 hand, *in situ*-produced  $^{14}\text{C}$ , with its short half-life, is able to reveal short-term sediment storage time  
932 within large floodplains (Hippe et al., 2012). These values can be compared with long-term estimates  
933 of sediment production when they are used in combination with  $^{10}\text{Be}$  and  $^{26}\text{Al}$  (Hippe et al., 2012).  
934 Also, coupling  $^{21}\text{Ne}$  concentrations with the nuclide pair  $^{10}\text{Be}$  and  $^{26}\text{Al}$ , all measured in the same

935 quartz-bearing material, improves both the accuracy and the time range of  $^{26}\text{Al}/^{10}\text{Be}$  burial dating  
936 (Balco and Shuster, 2009).

## 937 **7. Application of multiple numerical dating methods to single fluvial sequences**

938 In this contribution, we have focused on the major recent developments of five numerical dating  
939 techniques and showed how these have enabled new dating applications in diverse fluvial settings at  
940 different time scales. However, two main recommendations must be borne in mind. First, there is no  
941 ideal numerical dating method that can provide accurate age results on any kind of sample and in any  
942 context. The use of a dating method, even the most established one such as  $^{14}\text{C}$ , is limited by a range  
943 of intrinsic constraints and based on some implicit assumptions. Because the latter are rarely openly  
944 stated, expectations regarding numerical dating methods from non-geochronologists are sometimes  
945 unreasonable. Setting more realistic expectations from non-specialists is a key aim of this paper.  
946 Second, each method presented here, when applied to fluvial archives or landforms, may encounter  
947 specific methodological issues. This, in turn, may bias the “true” age of the event that has to be dated:  
948 for instance, age overestimation of a fluvial depositional event may be caused by the reworking of  
949 organic material ( $^{14}\text{C}$ ), incomplete bleaching of the quartz dosimeter (OSL and ESR), inaccurate  
950 estimation of the initial ( $^{230}\text{Th}/^{232}\text{Th}$ ) activity ratio ( $^{230}\text{Th}/\text{U}$ ) or inherited nuclide concentrations (TCN).

951 To overcome some of these limitations, we therefore strongly recommend applying three different  
952 approaches. Each of these is exemplified by case studies, including a discussion how the combination  
953 of these dating methods may strengthen the chronological framework of fluvial archives. First,  
954 provided that the petrographic composition of the fluvial sediments is favourable, some of these dating  
955 methods may allow an internal cross-check. For instance, surface exposure ages are strengthened  
956 when  $^{10}\text{Be}$  concentrations are measured alongside  $^{36}\text{Cl}$  concentrations from quartz-bearing and  
957 calcite-bearing material, respectively (e.g. Le Dortz et al., 2011). The same holds for luminescence  
958 dating: Colarossi et al. (2015) comparatively analysed OSL (quartz) and post-IR IRSL (feldspar)  
959 signals from identical samples collected in Quaternary river sediments (South Africa) to test whether  
960 the second dosimeter can reliably date partially bleached sediments. Notwithstanding the statement  
961 that the post-IR IRSL<sub>225</sub> signal was the most adequate because of the fastest bleaching kinetics, age  
962 convergence and divergence were both observed for younger (<20 ka) and older (>50 ka) samples,  
963 respectively (Colarossi et al., 2015 ). Further research is however required to understand the cause(s)  
964 of this discrepancy for older fluvial material.

965 Second, as stated by Brauer et al. (2014), it is of major importance to produce independent  
966 chronologies obtained from different dating methods, provided that the nature and the characteristics  
967 of the fluvial deposits allows it (e.g. Table 1). A common combination involves radiocarbon and OSL  
968 dating to yield robust chronologies for Late Pleistocene/Holocene fluvial sequences (e.g. de Moor et  
969 al., 2008). Moreover, age discrepancies between these two dating methods may give further insights  
970 into methodological issues. For instance, based on directly comparable paired OSL and  $^{14}\text{C}$  ages of  
971 Late Pleistocene terrace deposits from Eastern England, Briant and Bateman (2009) showed that  
972 ages inferred from both methods are either consistent (<29-35 ka) or divergent (>29-35 ka) (Fig. 9a).  
973 The systematic age underestimation of  $^{14}\text{C}$  dating beyond this limit is attributed to secondary  
974 contamination of older organic material by low levels of modern carbon (Fig. 3); it was thus suggested  
975 that conventionally pre-treated  $^{14}\text{C}$  ages  $\geq 29$ -35 ka should be treated with great caution (Briant and  
976 Bateman, 2009). Likewise, some of the case studies mentioned in this contribution take advantage of  
977 rarely used combinations between OSL, ESR,  $^{230}\text{Th}/\text{U}$  and TCN dating (Chaussé et al., 2004; Stock et  
978 al., 2005; Kock et al., 2009; Le Dortz et al., 2011; Blisniuk et al. 2012). For instance, Blisniuk et al.  
979 (2012) applied a combination of  $^{10}\text{Be}$  exposure dating with  $^{230}\text{Th}/\text{U}$ -dating to constrain the deposition of  
980 mid-Holocene to late Pleistocene alluvial fans (California). Three sampling strategies were  
981 implemented for the first method: top surface of individual large boulders (Fig. 7a), amalgamate of  
982 surface clasts and depth profile (Fig. 7c). The second method involved the sampling of post-  
983 depositional pedogenic carbonate from sub-surface clast-coatings.  $^{230}\text{Th}/\text{U}$  ages (minimum ages) are  
984 convergent or slightly younger than TCN ages (maximum ages if not corrected for inheritance and  
985 assuming zero denudation), thereby proving the usefulness of this combined approach in obtaining  
986 reliable depositional ages of fan deposits (Fig. 9b). Furthermore, the computing of  $^{10}\text{Be}$  depth profile  
987 ages of Late Pleistocene alluvium was made easier by the valuable minimum age information inferred  
988 from  $^{230}\text{Th}/\text{U}$  dating (Fig. 9b).

989 Third, as well as the parallel use of two or more independent methods from the same fluvial  
990 sequences, a few exploratory studies have attempted to merge the dating principles of distinct  
991 methods. For instance, Guralnik et al. (2011) developed an innovative approach using a mathematical  
992 framework for consistently incorporating  $^{10}\text{Be}$  concentration data along a depth profile with OSL ages  
993 from a single alluvial section (Fig. 9c, d). This model is based on three parameters and solves an  
994 integrated, co-dependent and self-consistent set of equations and assumes fluvial aggradation at a  
995 constant rate, with uniform cosmogenic inheritance, followed by terrace abandonment and subsequent

996 preservation and exposure of its surface (Fig. 9c, d). This scenario of terrace evolution may be  
997 validated or rejected by comparing model depth concentration data and model OSL ages to real  
998 observations (Guralnik et al., 2011).

999 As a conclusion, establishing reliable chronologies for Quaternary fluvial sequences has strongly  
1000 benefited from such applications of multiple dating methods. We finally recommend combining age  
1001 results of numerical methods with chronological information obtained from relative dating methods.  
1002 This is particularly well exemplified by the study of Antoine et al. (2007), synthesizing age results in  
1003 the Somme valley (northern France), where diverse numerical ( $^{14}\text{C}$ , TL, IRSL, ESR,  $^{230}\text{Th}/\text{U}$ ) and  
1004 relative (palaeomagnetism, mammalian biostratigraphy and amino-acid racemization) methods were  
1005 implemented. In addition, control for ESR dating was internally provided by cross-checking results of  
1006 optically bleached quartz grains with U-series/ESR dating of tooth enamel. This multi-dating approach  
1007 enabled Antoine et al. (2007) to build a coherent and robust chronostratigraphical interpretation of the  
1008 terrace sequence of the Somme valley for the last 1 Ma.

1009

#### 1010 **Acknowledgements**

1011 M. Duval's research was funded by a Marie Curie International Outgoing Fellowship of the EU's  
1012 Seventh Framework Programme (FP7/2007-2013), awarded under REA Grant Agreement No. PIOF-  
1013 GA-2013-626474. D. Scholz acknowledges funding of the DFG (SCHO 1274/9-1). Two anonymous  
1014 reviewers are acknowledged for their thoughtful suggestions on an earlier version of this manuscript.  
1015 David Bridgland is also acknowledged for his editorial work and for having improved the English of the  
1016 manuscript.

#### 1017 **References**

- 1018 Adams, K.D., Locke, W.W., Rossi, R., 1992. Obsidian-hydration dating of fluvially reworked sediments in the West  
1019 Yellowstone region, Montana. *Quaternary Research* 38, 180-195.
- 1020 Adamson, K.R., Woodward, J.C., Hughes, P.D., 2014. Glaciers and rivers: Pleistocene uncoupling in a  
1021 Mediterranean mountain karst. *Quaternary Science Reviews* 94, 28-43.
- 1022 Aitken, M.J. 1985. *Thermoluminescence dating*. Academic Press, London.
- 1023 Anderson, R.S., Repka, J.L., Dick, G.S., 1996. Explicit treatment of inheritance in dating depositional surfaces  
1024 using in situ  $^{10}\text{Be}$  and  $^{26}\text{Al}$ . *Geology* 24, 47-51.
- 1025 Anthony, D.M., Granger, D.E., 2007. A new chronology for the age of Appalachian erosional surfaces determined  
1026 by cosmogenic nuclides in cave sediments. *Earth Surface Process and Landforms* 887, 874-887.

1027 Antoine, P., Limondin Lozouet, N., Chaussé, C., Lautridou, J.-P., Pastre, J.-F., Auguste, P., Bahain, J.-J.,  
1028 Falguères, C., Galehb, B., 2007. Pleistocene fluvial terraces from northern France (Seine, Yonne, Somme):  
1029 synthesis, and new results from interglacial deposits. *Quaternary Science Reviews* 26(22–24), 2701-2723.

1030 Antón, L., Rodés, A., De Vicente, G., Pallàs, R., Garcia-Castellanos, D., Stuart, F.M., Braucher, R., Bourlès, D.,  
1031 2012. Quantification of fluvial incision in the Duero Basin (NW Iberia) from longitudinal profile analysis and  
1032 terrestrial cosmogenic nuclide concentrations. *Geomorphology* 165-166, 50–61.

1033 Arnold, L.J., Roberts, R.G., 2009. Stochastic modelling of multi-grain equivalent dose (De) distributions:  
1034 implications for OSL dating of sediment mixtures. *Quaternary Science Reviews* 4, 209-230.

1035 Arnold, L.J., Demurob, M., Parésc, J.M., Pérez-González, A., Arsuagad, J.L., Bermúdez de Castro, J.M.,  
1036 Carbonell, E., 2015. Evaluating the suitability of extended-range luminescence dating techniques over early and  
1037 Middle Pleistocene timescales: Published datasets and case studies from Atapuerca, Spain. *Quaternary*  
1038 *International* 389, 167–190.

1039 Balco, G., Rovey, C.W., 2008. An isochron method for cosmogenic-nuclide dating of buried soils and sediments.  
1040 *American Journal of Science* 308, 1083–1114.

1041 Balco, G., Shuster, D.L., 2009.  $^{26}\text{Al}$ - $^{10}\text{Be}$ - $^{21}\text{Ne}$  burial dating. *Earth and Planetary Science Letters* 286, 570–575.

1042 Bartz, M., Klasen, N., Zander, A., Brill, D., Rixhon, G., Seeliger, M., Eiwanger, J., Weniger, G.-C., Mikdad, A.,  
1043 Brückner, H., 2015. Luminescence dating of ephemeral stream deposits around the Palaeolithic site of Ifri  
1044 n'Ammar (Morocco). *Quaternary Geochronology* 30, 460-465.

1045 Bates, M.R., 1994. Quaternary aminostratigraphy in northwestern France. *Quaternary Science Reviews* 12, 793–  
1046 809.

1047 Baynes, E.R.C., Attal, M., Niedermann, S., Kirstein, L.A., Dugmore, A.J., Naylor, M., 2015. Erosion during  
1048 extreme flood events dominates Holocene canyon evolution in northeast Iceland. *Proceedings of the National*  
1049 *Academy of Sciences* 112, 2355-2360.

1050 Beerten, K., Stesmans, A., 2006. Some properties of Ti-related paramagnetic centres relevant for electron spin  
1051 resonance dating of single sedimentary quartz grains. *Applied Radiation and Isotopes* 64, 594-602.

1052 Bird, M.I., Ayliffe, L.K., Fifield, L.K., Turney, C.M., Cresswell, R.G., Barrows, T.T., David, B., 1999. Radiocarbon  
1053 dating of "old" charcoal using a wet oxidation, stepped-combustion procedure. *Radiocarbon* 41, 127-140.

1054 Bischoff, J.L., Fitzpatrick, J.A., 1991. U-series dating of impure carbonates: An isochron technique using total-  
1055 sample dissolution. *Geochimica et Cosmochimica Acta* 55, 543-554.

1056 Blisniuk, K., Oskin, M., Fletcher, K., Rockwell, T., Sharp, W., 2012. Assessing the reliability of U-series and  $^{10}\text{Be}$   
1057 dating techniques on alluvial fans in the Anza Borrego Desert, California. *Quaternary Geochronology* 13, 26-41.

1058 Blisniuk, P.M. and Sharp, W.D., 2003. Rates of late Quaternary normal faulting in central Tibet from U-series  
1059 dating of pedogenic carbonate in displaced fluvial gravel deposits. *Earth and Planetary Science Letters* 215, 169-  
1060 186.

1061 Bourdon, B., Henderson, G.M., Lundstrom, C.C., Turner, S.P. (Eds.), 2003. Uranium-series Geochemistry.  
1062 Mineralogical Society of America, Washington, DC.

1063 Braucher, R., Del Castillo, P., Siame, L., Hidy, A.J., Bourlès, D.L., 2009. Determination of both exposure time and  
1064 denudation rate from an in situ-produced  $^{10}\text{Be}$  depth profile: A mathematical proof of uniqueness. Model  
1065 sensitivity and applications to natural cases. *Quaternary Geochronology* 4, 56–67.

1066 Brauer, A., Hajdas, I., Blockley, S.P., Ramsey, C.B., Christl, M., Ivy-Ochs, S., Moseley, G.E., Nowaczyk, N.N.,  
1067 Rasmussen, S.O., Roberts, H.M., Spötl, C., 2014. The importance of independent chronology in integrating  
1068 records of past climate change for the 60–8 ka INTIMATE time interval. *Quaternary Science Reviews* 106, 47-66.

1069 Briant, R.M., Coope, G.R., Preece, R.C., Gibbard, P.L., 2004. Evidence for early Devensian (Weichselian) fluvial  
1070 sedimentation: Geochronological and palaeoenvironmental data from the Upper Pleistocene deposits at Deeping  
1071 St James, Lincolnshire, England. *Quaternaire* 15, 5–15.

1072 Briant, R.M., Bates, M.R., Schwenninger, J-L., Wenban-Smith, F.F. 2006. A long optically-stimulated  
1073 luminescence dated Middle to Late Pleistocene fluvial sequence from the western Solent Basin, southern  
1074 England. *Journal of Quaternary Science* 21, 507-523.

1075 Briant, R.M., Bateman, M.D., 2009. Luminescence dating indicates radiocarbon age underestimation in late  
1076 Pleistocene fluvial deposits from eastern England. *Journal of Quaternary Science* 24, 916-927.

1077 Brock, F., Higham, T., Ditchfield, P., Bronk Ramsey, C., 2010. Current pretreatment methods for AMS  
1078 radiocarbon dating at the Oxford Radiocarbon Accelerator Unit (ORAU). *Radiocarbon* 52, 103-112.

1079 Broecker, W.S., 1963. A preliminary evaluation of uranium series inequilibrium as a tool for absolute age  
1080 measurement on marine carbonates. *Journal of Geophysical Research* 68, 2817-2834.

1081 Brunnacker, K., Löscher, M., Tillmanns, W., Urban, B., 1982. Correlation of the Quaternary terrace sequence in  
1082 the lower Rhine Valley and northern Alpine foothills of Central Europe. *Quaternary Research* 18, 152–173.

1083 Burbank D.W., Leland, J., Fielding, E., Anderson, R.S., Brozovic, N., Reid, M.R., Duncan, C., 1996. Bedrock  
1084 incision, rock uplift & threshold hillslopes in NW Himalayas. *Nature* 379, 505–510.

1085 Buylaert, J.P., Murray, A.S., Thomsen, K.J., Jain, M., 2009. Testing the potential of an elevated temperature  
1086 IRSL signal from K-feldspar. *Radiation Measurements* 44, 560-565.

1087 Candy, I., Black, S., Sellwood, B.W., 2004. Quantifying time scales of pedogenic calcrete formation using U-  
1088 series disequilibria. *Sedimentary Geology* 170, 177-187.

1089 Candy, I., Black, S., Sellwood, B.W., 2005. U-series isochron dating of immature and mature calcretes as a basis  
1090 for constructing Quaternary landform chronologies for the Sorbas basin, southeast Spain. *Quaternary Research*  
1091 64, 100-111.

1092 Candy, I., Schreve, D., 2007. Land-sea correlation of Middle Pleistocene temperate sub-stages using high-  
1093 precision uranium-series dating of tufa deposits from southern England. *Quaternary Science Reviews* 26, 1223-  
1094 1235.

1095 Chaussé, C., Voinchet, P., Bahain, J.J., Connet, N., Lhomme, V., Limondin-Lozouet, N., 2004. Middle and upper  
1096 Pleistocene evolution of the river Yonne valley (France). *Quaternaire* 15, 53–64.

1097 Cheng, H., Edwards, R.L., Hoff, J., Gallup, C.D., Richards, D.A., Asmerom, Y., 2000. The half-lives of uranium-  
1098 <sup>234</sup> and thorium-230. *Chemical Geology* 169, 17-33.

1099 Cheng, H., Edwards, R.L., Shen, C.-C., Polyak, V.J., Asmerom, Y., Woodhead, J., Hellstrom, J., Wang, Y., Kong,  
1100 X., Spötl, C., Wang, X., Alexander Jr., E.C., 2013. Improvements in <sup>230</sup>Th dating, <sup>230</sup>Th and <sup>234</sup>U half-life values,  
1101 and U-Th isotopic measurements by multi-collector inductively coupled plasma mass spectrometry. *Earth and*  
1102 *Planetary Science Letters* 371, 82-91.

1103 Colarossi D., Duller G.A.T., Roberts H.M., Tooth S., Lyons R., 2015. Comparison of paired quartz OSL and  
1104 feldspar post-IR IRSL dose distributions in poorly bleached fluvial sediments from South Africa. *Quaternary*  
1105 *Geochronology* 30, 233-238.

1106 Colman, S.M., Pierce, K.L., 1981. Weathering rinds on andesitic and basaltic stones as a Quaternary Age  
1107 indicator, Western United States. *Geological Survey Professional Paper* 1210 1–56.

1108 Coltorti, M., Della Fazia, J., Paredes Rios, F., Tito, G., 2010. The Nuagapua alluvial fan sequence: Early and Late  
1109 Holocene human-induced changes in the Bolivian Chaco? *Proceedings of the Geologists' Association* 121, 218–  
1110 228.

1111 Cordier, S., Harmand, D., Lauer, T., Voinchet, P., Bahain, J.-J., Frechen, M., 2012. Geochronological  
1112 reconstruction of the Pleistocene evolution of the Sarre valley (France and Germany) using OSL and ESR dating  
1113 techniques. *Geomorphology* 165–166, 91-106.

1114 Cordier, S., Frechen, M., Harmand, D., 2014. Dating fluvial erosion: Fluvial response to climate change in the  
1115 Moselle catchment (France, Germany) since the Late Saalian. *Boreas* 43, 450–468.

1116 Crook, R., 1986. Relative dating of Quaternary deposits based on P-wave velocities in weathered granitic clasts.  
1117 *Quaternary Research* 25, 281–292.

1118 Cunha, P.P., Almeida, N.A.C., Aubry, T., Martins, A.A., Murray, A.S., Buylaert, J.P., Sohbaty, R., Raposo, L.,  
1119 Rocha, L., 2012. Records of human occupation from Pleistocene river terrace and aeolian sediments in the  
1120 Arneiro depression (Lower Tejo River, central eastern Portugal). *Geomorphology* 165-166, 78–90.

1121 Cunningham, A.C., Wallinga, J., 2010. Selection of integration time intervals for quartz OSL decay  
1122 curves. *Quaternary Geochronology* 5, 657-666.

1123 Cunningham A.C., Wallinga, J., 2012. Realizing the potential of fluvial archives using robust OSL chronologies.  
1124 *Quaternary Geochronology* 12, 98-106.

1125 Darling, A.L., Karlstrom, K.E., Granger, D.E., Aslan, A., Kirby, E., Ouimet, W.B., Lazear, G.D., Coblenz, D.D.,  
1126 Cole, R.D., 2012. New incision rates along the Colorado River system based on cosmogenic burial dating of  
1127 terraces: Implications for regional controls on Quaternary incision. *Geosphere* 8, 1020–1041.

1128 Davis, W.M., 1899. The geographical cycle. *Geogr. J.* 481–504.

1129 Davis, R., Schaeffer, O.A., 1955. Chlorine-36 in nature. *Ann. NY Acad. Sc.* 62, 105-122.

1130 Deevey Jr, E.S., Gross, M.S., Hutchinson, G.E. and Kraybill, H.L., 1954. The natural C14 contents of materials  
1131 from hard-water lakes. *Proceedings of the National Academy of Sciences* 40, 285.

1132 de Moor, J.J.W., Kasse, C., van Balen, R., Vandenberghe, J., Wallinga, J., 2008. Human and climate impact on  
1133 catchment development during the Holocene - Geul River, the Netherlands. *Geomorphology* 98, 316–339.

1134 Despriée, J., Gageonnet, R., Voinchet, P., Bahain, J.J., Falguères, C., Duvalard, J., Varache, F., 2004.  
1135 Pleistocene fluvial systems of the Creuse River (Middle Loire Basin - Centre Region, France). *Quaternaire* 15,  
1136 77–86.

1137 Ditlefsen, C., 1992. Bleaching of K-feldspars in turbid water suspensions: A comparison of photo- and  
1138 thermoluminescence signals. *Quaternary Science Reviews* 11, 33-38.

1139 Dunai, T., 2010. *Cosmogenic nuclides - Principles, Concepts and Applications in the Earth Surface Sciences*,  
1140 Cambridge University Press, 187p.

1141 Duller, G.A.T., 2004. Luminescence dating of Quaternary sediments: recent advances. *Journal of Quaternary*  
1142 *Science* 19, 183-192.

1143 Duller, G.A.T., 2008. Single-grain optical dating of Quaternary sediments: why aliquot size matters in  
1144 luminescence dating. *Boreas* 37, 589-612.

1145 Duval, M., 2012. Dose response curve of the ESR signal of the Aluminum center in quartz grains extracted from  
1146 sediment. *Ancient TL* 30, 1-9.

1147 Duval, M., 2015. Electron Spin Resonance (ESR) Dating of Fossil Tooth Enamel. *Encyclopedia of Scientific*  
1148 *Dating Methods*. W. J. Rink and J. W. Thompson, Springer Netherlands, 239-246.

1149 Duval, M. (2016). Electron Spin Resonance Dating in Archaeology. In: Gilbert A.S. (Ed.) *Encyclopedia of*  
1150 *Geoarchaeology*. Springer. DOI: 10.1007/978-1-4020-4409-0.

1151 Duval, M., Guilarte Moreno, V., 2012. Assessing the influence of the cavity temperature on the ESR signal of the  
1152 Aluminum center in quartz grains extracted from sediment. *Ancient TL* 30, 11-16.

1153 Duval, M, Guilarte V., 2012. ESR dosimetry of optically bleached quartz grains extracted from Plio-Quaternary  
1154 sediment: Evaluating some key aspects of the ESR signals associated to the Ti-centers. *Radiation Measurements*  
1155 78, 28-41.

1156 Duval, M., Sancho, C., Calle, M., Guilarte, V., Peña-Monné, J.L., 2015. On the interest of using the multiple center  
1157 approach in ESR dating of optically bleached quartz grains: Some examples from the Early Pleistocene terraces  
1158 of the Alcanadre River (Ebro basin, Spain). *Quaternary Geochronology* 29, 58-69.

1159 Edwards, R.L., Chen, J.H., Wasserburg, G. J., 1987.  $^{238}\text{U}$ - $^{234}\text{U}$ - $^{230}\text{Th}$ - $^{232}\text{Th}$  systematics and the precise  
1160 measurement of time over the past 500,000 years. *Earth and Planetary Science Letters* 81, 175-192.

1161 Edwards, R.L., Gallup, C.D., Cheng, H., 2003. Uranium-series dating of marine and lacustrine carbonates. In:  
1162 Bourdon, B., Henderson, G.M., Lundstrom, C.C., and Turner, S. P. Eds.), *Uranium-series Geochemistry*.  
1163 Mineralogical Society of America, Washington, DC.

1164 Eggins, S.M., Grün, R., McCulloch, M.T., Pike, A.W.G., Chappell, J., Kinsley, L., Mortimer, G., Shelley, M.,  
1165 Murray-Wallace, C.V., Spötl, C., Taylor, L., 2005. In situ U-series dating by laser-ablation multi-collector ICPMS:  
1166 new prospects for Quaternary geochronology. *Quaternary Science Reviews* 24, 2523-2538.

1167 Engel, S.A., Gardner, T.W., Ciolkosz, E.J., 1996. Quaternary soil chronosequences on terraces of the  
1168 Susquehanna River, Pennsylvania. *Geomorphology* 17, 273–294.

1169 Erlanger, E.D., Granger, D.E., Gibbon, R.J., 2012. Rock uplift rates in South Africa from isochron burial dating of  
1170 fluvial and marine terraces. *Geology* 40, 1019–1022.

1171 Falguères, C., Bahain, J.-J., Pérez-González, A., Mercier, N., Santonja, M., Dolo, J.-M., 2006. The Lower  
1172 Acheulian site of Ambrona, Soria (Spain): ages derived from a combined ESR/U-series model. *Journal of*  
1173 *Archaeological Science* 33, 149-157.

1174 Flez, C., Lahousse, P., 2015. Example of Holocene alpine torrent response to environmental change : contribution  
1175 to assessment of forcing factors. *Quaternaire* 15, 167–176.

1176 Fontana, A., Mozzi, P., Bondesan, A., 2008. Alluvial megafans in the Venetian-Friulian Plain (north-eastern Italy):  
1177 Evidence of sedimentary and erosive phases during Late Pleistocene and Holocene. *Quaternary International*  
1178 189, 71–90.

1179 Fuchs, M.C., Kreuzer, S., Burow, C., Dietze, M., Fischer, M., Schmidt, C., Fuchs, M., 2015. Data processing in  
1180 luminescence dating analysis: An exemplary workflow using the R package 'Luminescence'. *Quaternary*  
1181 *International* 362, 8-13.

1182 Galbraith, R.F., 2010. On plotting OSL equivalent dose estimates. *Ancient TL* 28, 1-9.

1183 Galbraith, R.F., Green, P.F., 1990. Estimating the component ages in a finite mixture. *Nuclear Tracks and*  
1184 *Radiation Measurements* 17, 197-206.

1185 Galbraith, R.F., Laslett, G.M., 1993. Statistical models for mixed fission track ages. *Nuclear Tracks and Radiation*  
1186 *Measurements* 21, 495-470.

1187 Galbraith, R.F., Roberts, R.G., 2012. Statistical aspects of equivalent dose and error calculation and display in  
1188 OSL dating: an overview and some recommendations. *Quaternary Geochronology* 11, 1-27.

1189 Garnier, A., Lespez, L., Ozainne, S., Ballouche, A., Mayor, A., Le Drézen, Y., Rasse, M., Huysecom, E., 2015.  
1190 L'incision généralisée de la vallée du Yamé (Mali) entre 2 350 et 1 700 ans cal. BP : quelle signification  
1191 paléoenvironnementale et archéologique? *Quaternaire* 26, 49-66.

1192 Geach, M.R., Thomsen, K.J., Buylaert, J.-P., Murray, A.S., Mather, A.E., Telfer, M.W., Stokes, M., 2015. Single-  
1193 grain and multi-grain OSL dating of river terrace sediments in the Tabernas Basin, SE Spain. *Quaternary*  
1194 *Geochronology* 30, 213-218

1195 Godwin, H., 1962. Half-life of radiocarbon. *Nature* 195.

1196 Goldstein, S.J., Stirling, C.H., 2003. Techniques for measuring Uranium-series nuclides: 1992-2002. In: Bourdon,  
1197 B., Henderson, G.M., Lundstrom, C.C., and Turner, S.P. Eds.), *Uranium-series Geochemistry*. Mineralogical  
1198 Society of America, Washington, DC.

1199 Gosse, J.C., Phillips, F.M., 2001. Terrestrial in situ cosmogenic nuclides: theory and application. *Quaternary*  
1200 *Science Reviews* 20, 1475–1560.

1201 Gorter, S.C., 1936. Paramagnetic relaxation in a transversal magnetic field. *Physica* 3, 1006–1008.

1202 Granger, D.E., Kirchner, J.W., Finkel, R.C., 1997. Quaternary downcutting rate of the New River, Virginia,  
1203 measured from differential decay of cosmogenic  $^{26}\text{Al}$  and  $^{10}\text{Be}$  in cave-deposited alluvium. *Geology* 25, 107–110.

1204 Granger, D.E., Muzikar, P.F., 2001. Dating sediment burial with in situ-produced cosmogenic nuclides: theory,  
1205 techniques, and limitations. *Earth and Planetary Science Letters* 188, 269–281.

1206 Granger, D.E., 2014. Cosmogenic Nuclide Burial Dating in Archaeology and Paleoanthropology, in: *Treatise on*  
1207 *Geochemistry: Second Edition*. Elsevier Ltd., pp. 81–97.

1208 Grün, R., 1989. Electron spin resonance (ESR) dating. *Quaternary International* 1(0), 65-109.

1209 Grün, R., 2000. An alternative model for open system U-series/ESR age calculations: (closed system U-series)-  
1210 ESR, CSUS-ESR. *Ancient TL* 18(1), 1-4.

1211 Grün, R., 2009. The relevance of parametric U-uptake models in ESR age calculations. *Radiation Measurements*  
1212 44(5–6), 472-476.

1213 Grün, R., Schwarcz, H.P., Chadam, J., 1988. ESR dating of tooth enamel: Coupled correction for U-uptake and  
1214 U-series disequilibrium. *Nuclear Tracks and Radiation Measurements* 14, 237-241

1215 Guerin, G., Combès, B., Lahaye, C., Thomsen, K.J., Tribolo, C., Urbanova, P., Guibert, P., Mercier, N., Valladas,  
1216 H., 2015. Testing the accuracy of a Bayesian central-dose model for single-grain OSL, using known-age samples.  
1217 *Radiation Measurements* 81, 62-70.

1218 Guilarte, V., Trompier, F., Duval, M. Evaluating the potential of Q-band ESR spectroscopy for dose reconstruction  
1219 of fossil tooth enamel. *PLoS ONE* 11(3): e0150346. DOI:10.1371/journal.pone.0150346.

1220 Guralnik, B., Matmon, A., Avni, Y., Porat, N., Fink, D., 2011. Constraining the evolution of river terraces with  
1221 integrated OSL and cosmogenic nuclide data. *Quaternary Geochronology* 6, 22–32.

1222 Harmand, D., Voinchet, P., Cordier, S., Bahain, J., Rixhon, G., 2015. Datations ESR de terrasses alluviales des  
1223 vallées de la Moselle et de la Meurthe (France, Allemagne): implications chronostratigraphiques et limites  
1224 méthodologiques. *Quaternaire*, 13–26.

1225 Häuselmann, P., Granger, D.E., Jeannin, P.-Y., Lauritzen, S.-E., 2007. Abrupt glacial valley incision at 0.8 Ma  
1226 dated from cave deposits in Switzerland. *Geology* 35, 143–146.

1227 Hellstrom, J.C., 2006. U-Th dating of speleothems with high initial  $^{230}\text{Th}$  using stratigraphical constraint.  
1228 *Quaternary Geochronology* 1, 289-295.

1229 Hidy, A.J., Gosse, J.C., Pederson, J.L., Mattern, J.P., Finkel, R.C., 2010. A geologically constrained Monte Carlo  
1230 approach to modeling exposure ages from profiles of cosmogenic nuclides: An example from Lees Ferry, Arizona.  
1231 *Geochemistry, Geophysics, Geosystems* 11.

1232 Higham, T.F., Jacobi, R.M., Ramsey, C.B., 2006. AMS radiocarbon dating of ancient bone using ultrafiltration.  
1233 *Radiocarbon* 48, 179.

- 1234 Hippe, K., Kober, F., Zeilinger, G., Ivy-Ochs, S., Maden, C., Wacker, L., Kubik, P.W., Wieler, R., 2012.  
1235 Quantifying denudation rates and sediment storage on the eastern Altiplano, Bolivia, using cosmogenic  $^{10}\text{Be}$ ,  $^{26}\text{Al}$ ,  
1236 and *in situ*  $^{14}\text{C}$ . *Geomorphology* 179, 58–70.
- 1237 Hogg, A.G., Hua, Q., Blackwell, P.G., Niu, M., Buck, C.E., Guilderson, T.P., Heaton, T.J., Palmer, J.G., Reimer,  
1238 P.J., Reimer, R.W., Turney, C.S., 2013. SHCal13 Southern Hemisphere calibration, 0–50,000 years cal BP.  
1239 *Radiocarbon* 55, 1889-1903.
- 1240 Huntley, D.J., Godfrey-Smith, D.I., Thewalt, M.L., 1985. Optical dating of sediments. *Nature* 313, 105-107.
- 1241 Huntley, D.J., Lamothe, M., 2001. Ubiquity of anomalous fading in K-feldspars and the measurement and  
1242 correction for it in optical dating. *Canadian Journal of Earth Sciences* 38, 1093-1106.
- 1243 Ikeya, M., 1975. Dating a stalactite by electron paramagnetic resonance. *Nature* 255, 48-50.
- 1244 Ikeya, M., 1993. *New Applications of Electron Spin Resonance Dating, Dosimetry and Microscopy*. Singapore,  
1245 World Scientific.
- 1246 Ivanovich, M., & Harmon, R. S. (Eds.). (1992). *Uranium-series disequilibrium: Applications to earth, marine, and*  
1247 *environmental sciences*. Oxford University Press.
- 1248 Ivy-Ochs, S, Kober, F., 2008. Surface exposure dating with cosmogenic nuclides. *Eiszeitalter und Gegenwart –*  
1249 *Quaternary Science Journal* 57, 179-209.
- 1250 Jacobson, R.B., Elston, D.P., Heaton, J.W., 1988. Stratigraphy and magnetic polarity of the High Terrace  
1251 remnants in the Upper Ohio and Monongahela Rivers in West Virginia, Pennsylvania and Ohio. *Quaternary*  
1252 *Research* 29, 216–232.
- 1253 Jain, M., Murray, A.S., Botter-Jensen, L., 2004. Optically stimulated luminescence dating: How significant is  
1254 incomplete light exposure in fluvial environments? *Quaternaire* 15, 143–157.
- 1255 Jain, M., Murray, A.S., Bøtter-Jensen, L., Wintle, A.G., 2005. A single-aliquot regenerative-dose method based on  
1256 IR bleaching of the fast OSL component in quartz. *Radiation Measurements* 39, 309-318.
- 1257 Joannes-Boyau, R., Grün, R., 2011. A comprehensive model for  $\text{CO}_2^-$  radicals in fossil tooth enamel: Implications  
1258 for ESR dating. *Quaternary Geochronology* 6, 82-97.
- 1259 Kalicki, T., Sauchyk, S., Calderoni, G., Simakova, G., 2008. Climatic versus human impact on the Holocene  
1260 sedimentation in river valleys of different order: Examples from the upper Dnieper basin, Belarus. *Quaternary*  
1261 *International* 189, 91–105.
- 1262 Kasse, C., Bohncke, S.J.P., Vandenberghe, J., 1995. Fluvial periglacial environments, climate and vegetation  
1263 during the Middle Weichselian in the Northern Netherlands with special reference to the Hengelo Interstadial.  
1264 *Mededelingen Rijks Geologische Dienst* 52, 387-414.
- 1265 Kasse, C., Bohncke, S.J.P., Vandenberghe, J., Gábris, G., 2010. Fluvial style changes during the last glacial-  
1266 interglacial transition in the middle Tisza valley (Hungary). *Proceedings of the Geologists' Association* 121, 180–  
1267 194.

1268 Kaufman, A., 1993. An evaluation of several methods for determining  $^{230}\text{Th}/\text{U}$  ages in impure carbonates.  
1269 *Geochimica et Cosmochimica Acta* 57, 2303-2317.

1270 Kaufman, A., Broecker, W., 1965. Comparison of  $^{230}\text{Th}$  and  $^{14}\text{C}$  ages for carbonate materials from Lakes  
1271 Lahontan and Bonneville. *Journal of Geophysical Research* 70, 4039-4054.

1272 Keen-Zebert, A., Tooth, S., Rodnight, H., Duller, G.A.T., Roberts, H.M., Grenfell, M., 2013. [Late Quaternary  
1273 floodplain reworking and the preservation of alluvial sedimentary archives in unconfined and confined river valleys  
1274 in the eastern interior of South Africa](#). *Geomorphology* 185, 54-66

1275 Kelly, M., Black, S., Rowan, J.S., 2000. A calcrite-based U/Th chronology for landform evolution in the Sorbas  
1276 basin, southeast Spain. *Quaternary Science Reviews* 19, 995-1010.

1277 Klein, J., Middleton, R., Tang, H., 1982. Modifications of an FN tandem for quantitative  $^{10}\text{Be}$  Measurement.  
1278 *Nuclear Instruments and Methods in Physics Research* 193, 601–616.

1279 Knuepfer, P., 1988. Estimating ages of late Quaternary stream terraces from analysis of weathering rinds and  
1280 soils. *Geological Society of America Bulletin* 100, 1224–1236.

1281 Kock, S., Kramers, J.D., Preusser, F., Wetzel, A., 2009. Dating of Late Pleistocene terrace deposits of the River  
1282 Rhine using Uranium series and luminescence methods: Potential and limitations. *Quaternary Geochronology* 4,  
1283 363-373.

1284 Kong, P., Granger, D.E., Wu, F.Y., Caffee, M.W., Wang, Y.J., Zhao, X.T., Zheng, Y., 2009. Cosmogenic nuclide  
1285 burial ages and provenance of the Xigeda paleo-lake: Implications for evolution of the Middle Yangtze River.  
1286 *Earth and Planetary Science Letters* 278, 131–141.

1287 Kreutzer, S., Schmidt, C., Fuchs, M. C., Dietze, M., Fischer, M., Fuchs, M., 2012. Introducing an R package for  
1288 luminescence dating analysis. *Ancient TL* 30, 1-8.

1289 Ku, T.-L., Liang, Z.-C., 1984. The dating of impure carbonates with decay-series isotopes. *Nuclear Instruments  
1290 and Methods in Physics Research* 223, 563-571.

1291 Kuzucuoglu, C., Fontugne, M., Muralis, D., 2004. Holocene terraces in the middle Euphrates valley, between  
1292 Halfeti and Karkemish (Gaziantep, Turkey). *Quaternaire* 15, 195–206.

1293 Lauer, T., Frechen, M., Hoselmann, C., Tsukamoto, S., 2010. Fluvial aggradation phases in the Upper Rhine  
1294 Graben-new insights by quartz OSL dating. *Proceedings of the Geologists' Association* 121, 154–161.

1295 Le Dortz, K., Meyer, B., Sébrier, M., Braucher, R., Nazari, H., Benedetti, L., Fattahi, M., Bourlès, D., Foroutan, M.,  
1296 Siame, L., Rashidi, A., Bateman, M.D., 2011. Dating inset terraces and offset fans along the Dehshir Fault (Iran)  
1297 combining cosmogenic and OSL methods. *Geophysical Journal International* 185, 1147–1174.

1298 Leland, J., Reid, M.R., Burbank, D.W., Finkel, R., Caffee, M., 1998. Incision and differential bedrock uplift along  
1299 the Indus River near Nanga Parbat, Pakistan Himalaya, from  $^{10}\text{Be}$  and  $^{26}\text{Al}$  exposure age dating of bedrock  
1300 straths. *Earth and Planetary Science Letters* 154, 93–107.

1301 Lewin, J., Macklin, M.G., 2003. Preservation potential for Late Quaternary river alluvium. *Journal of Quaternary  
1302 Science* 18, 107-120.

1303 Lewin, J., Macklin, M.G., Johnstone, E., 2005. Interpreting alluvial archives: sedimentological factors in the British  
1304 Holocene fluvial record. *Quaternary Science Reviews* 24, 1873-1889.

1305 Libby, W.F., Anderson, E.C., Arnold, J.R., 1949. Age determination by radiocarbon content: world-wide assay of  
1306 natural radiocarbon. *Science* 109, 227-228.

1307 Liu, C.-R., Grün, R., 2011. Fluvio-mechanical resetting of the Al and Ti centres in quartz. *Radiation*  
1308 *Measurements* 46(10): 1038-1042.

1309 Ludwig, K.R., 2003. Mathematical-statistical treatment of data and errors for  $^{230}\text{Th}/\text{U}$  geochronology. In: Bourdon,  
1310 B., Henderson, G.M., Lundstrom, C.C., and Turner, S.P. Eds.), *Uranium-series Geochemistry*. Mineralogical  
1311 Society of America, Washington, DC.

1312 Ludwig, K.R., Paces, J.B., 2002. Uranium-series dating of pedogenic silica and carbonate, Crater Flat, Nevada.  
1313 *Geochimica et Cosmochimica Acta* 66, 487-506.

1314 Luo, S., Ku, T.-L., 1991. U-series isochron dating: A generalized method employing total-sample dissolution.  
1315 *Geochimica et Cosmochimica Acta* 55, 555-564.

1316 Macklin, M.G., Johnstone, E., Lewin, J., 2005. Pervasive and long-term forcing of Holocene river instability and  
1317 flooding in Great Britain by centennial-scale climate change. *Holocene* 15, 937-943.

1318 Macklin, M.G., Jones, A.F., Lewin, J., 2010. River response to rapid Holocene environmental change: evidence  
1319 and explanation in British catchments. *Quaternary Science Reviews* 29, 1555-1576.

1320 Macklin, M.G., Lewin, J., 2003. River sediments, great floods and centennial-scale Holocene climate change.  
1321 *Journal of Quaternary Science* 18, 101-105.

1322 Martin, L., Incerti, S., Mercier, N., 2015. DosiVox: Implementing Geant 4-based software for dosimetry simulations  
1323 relevant to luminescence and ESR dating techniques. *Ancient TL* 33, 1-10.

1324 Martins, A.A., Cunha, P.P., Rosina, P., Osterbeek, L., Cura, S., Grimaldi, S., Gomes, J., Buylaert, J.P., Murray,  
1325 A.S., Matos, J., 2010. Geoarchaeology of Pleistocene open-air sites in the Vila Nova da Barquinha-Santa Cita  
1326 area (Lower Tejo River basin, central Portugal). *Proceedings of the Geologists' Association* 121, 128–140.

1327 Mathieu, J., Weisrock, A., Wengler, L., Brochier, J.E., Even, G., Fontugne, M., Mercier, N., Ouammou, A.,  
1328 Sénégas, F., Valladas, H., Vernet, J.L., Wahl, L., 2015. Holocene deposits in the lower section of the Assaka  
1329 Wadi, South Morocco: preliminary results. *Quaternaire* 15, 207–218.

1330 Mertz-Kraus, R., Jochum, K.P., Sharp, W.D., Stoll, B., Weis, U., Andreae, M.O., 2010. In situ  $^{230}\text{Th}$ - $^{232}\text{Th}$ - $^{234}\text{U}$ -  
1331  $^{238}\text{U}$  analysis of silicate glasses and carbonates using laser ablation single-collector sector-field ICP-MS. *Journal*  
1332 *of Analytical Atomic Spectrometry* 25, 1895-1904.

1333 Millard, A., 2014. Conventions for reporting radiocarbon determinations. *Radiocarbon* 56, 555–559.

1334 Mol, J., Roebroeks, W., Kamermans, H., van Kolfschoten, T., Turq, A., 2004. Weichselian and holocene fluvial  
1335 evolution of the Vézère river valley (Dordogne, France). *Quaternaire* 15, 187–193.

1336 Murray, A.S., Olley, J.M., 2002. Precision and accuracy in the optically stimulated luminescence dating of  
1337 sedimentary quartz: a status review. *Geochronometria* 21, 1-16.

1338 Murray, A.S., Wintle, A.G., 2000. [Luminescence dating of quartz using an improved single-aliquot regenerative-](#)  
1339 [dose protocol](#). Radiation Measurements 32, 57-73.

1340 Murray, A.S., Wintle, A.G., 2003. [The single aliquot regenerative dose protocol: potential for improvements in](#)  
1341 [reliability](#). Radiation Measurements 37, 377-381.

1342 Nishiizumi, K., Lal, D., Klein, J., Middleton, R., Arnold, J., 1986. Production of  $^{10}\text{Be}$  and  $^{26}\text{Al}$  by cosmic rays in  
1343 terrestrial quartz in situ and implications for erosion rates. Nature 319, 134-136.

1344 Owen, L. A., Clemmens, S.J., Finkel, R.C., Gray, H., 2014. Late Quaternary alluvial fans at the eastern end of the  
1345 San Bernardino Mountains, Southern California. Quaternary Science Reviews 87, 114–134.

1346 Penkman, K.E.H., Preece, R.C., Keen, D.H., Maddy, D., Schreve, D.C., Collins, M.J., 2007. Testing the  
1347 aminostratigraphy of fluvial archives: the evidence from intra-crystalline proteins within freshwater shells.  
1348 Quaternary Science Reviews 26, 2958–2969.

1349 Philippsen, B., 2013. The freshwater reservoir effect in radiocarbon dating. Heritage Science 1, 24.

1350 Pigati, J.S., Quade, J., Wilson, J., Jull, A.T., Lifton, N.A., 2007. Development of low-background vacuum  
1351 extraction and graphitization systems for  $^{14}\text{C}$  dating of old (40–60 ka) samples. Quaternary International 166, 4-  
1352 14.

1353 Preece, R.C., 1999. Mollusca from Last Interglacial fluvial deposits of the River Thames at Trafalgar Square,  
1354 London. Journal of Quaternary Science 14, 77–89.

1355 Preusser, F., Chithambo, M.L., Götze, T., Martini, M., Ramseier, K., Sendezera, E.J., Susino, G.J. and Wintle,  
1356 A.G., 2009. Quartz as a natural luminescence dosimeter. Earth-Science Reviews 97, 184-214.

1357 Rades, E.F., Hetzel, R., Xu, Q., Ding, L., 2013. Constraining holocene lake-level highstands on the tibetan  
1358 plateau by  $^{10}\text{Be}$  exposure dating: A case study at tangra yumco, southern tibet. Quaternary Science Reviews 82,  
1359 68–77.

1360 Ramos, A.M., Cunha, P.P., Cunha, L.S., Gomes, A., Lopes, F.C., Buylaert, J.P., Murray, A.S., 2012. The River  
1361 Mondego terraces at the Figueira da Foz coastal area (western central Portugal): Geomorphological and  
1362 sedimentological characterization of a terrace staircase affected by differential uplift and glacio-eustasy.  
1363 Geomorphology 165-166, 107–123.

1364 Reimer, P.J., Baillie, M.G., Bard, E., Bayliss, A., Beck, J.W., Bertrand, C.J., Blackwell, P.G., Buck, C.E., Burr,  
1365 G.S., Cutler, K.B., Damon, P.E., 2004. IntCal04 terrestrial radiocarbon age calibration, 0-26 cal kyr BP.  
1366 Radiocarbon 46, 1029-1058.

1367 Reimer, P.J., Bard, E., Bayliss, A., Beck, J.W., Blackwell, P.G., Bronk Ramsey, C., Buck, C.E., Cheng, H.,  
1368 Edwards, R.L., Friedrich, M., Grootes, P.M., 2013. IntCal13 and Marine13 Radiocarbon Age Calibration Curves  
1369 0–50,000 Years cal BP. Radiocarbon 55, 1869-1887.

1370 Repka, J.L., Anderson, R.S., Finkel, R.C., 1997. Cosmogenic dating of fluvial terraces, Fremont River, Utah.  
1371 Earth and Planetary Science Letters 152, 59–73.

1372 Reusser, L., Bierman, P., Pavich, M., Larsen, J., Finkel, R., 2006. An episode of rapid bedrock channel incision  
1373 during the last glacial cycle, measured with <sup>10</sup>Be. *American Journal of Science* 306, 69–102.

1374 Richards, D.A., Dorale, J.A., 2003. Uranium-series chronology and environmental applications of speleothems. In:  
1375 Bourdon, B., Henderson, G.M., Lundstrom, C.C., and Turner, S.P. Eds.), *Uranium-series Geochemistry*.  
1376 Mineralogical Society of America, Washington, DC.

1377 Rink, W. J., Bartoll, J., Schwarcz, H.P., Shane, P., Bar-Yosef, O., 2007. Testing the reliability of ESR dating of  
1378 optically exposed buried quartz sediments. *Radiation Measurements* 42, 1618-1626.

1379 Rittenour, T.M., 2008. Luminescence dating of fluvial deposits: applications to geomorphic, palaeoseismic and  
1380 archaeological research. *Boreas* 37, 613-635.

1381 Rixhon, G., Braucher, R., Bourlès, D., Siame, L., Bovy, B., Demoulin, A., 2011. Quaternary river incision in NE  
1382 Ardennes (Belgium) – Insights from <sup>10</sup>Be/<sup>26</sup>Al dating of river terraces. *Quaternary Geochronology* 6, 273–284.

1383 Rixhon, G., Bourlès, D.L., Braucher, R., Siame, L., Cordy, J.M., Demoulin, A., 2014. <sup>10</sup>Be dating of the Main  
1384 Terrace level in the Amblève valley (Ardennes, Belgium): New age constraint on the archaeological and  
1385 palaeontological filling of the Belle-Roche palaeokarst. *Boreas* 43, 528–542.

1386 Rodnight, H., 2008. How many equivalent dose values are needed to obtain a reproducible distribution? *Ancient*  
1387 *TL* 26, 3-10.

1388 Rogerson, R.J., Keen, D.H., Coope, G.R., Robinson, E., Dickson, J.H., Dickson, C.A., 1992. The fauna, flora and  
1389 palaeoenvironmental significance of deposits beneath the low terrace of the River Great Ouse at Radwell,  
1390 Bedfordshire, England. *Proceedings of the Geologists' Association* 103, 1-13.

1391 Roy-Barman, M. Pons-Branchu, E., 2016. Improved U-Th dating of carbonates with high initial <sup>230</sup>Th using  
1392 stratigraphical and coevality constraints. *Quaternary Geochronology* 32, 29-39.

1393 Ruff, M., Szidat, S., Gäggeler, H.W., Suter, M., Synal, H.A., Wacker, L., 2010. Gaseous radiocarbon  
1394 measurements of small samples. *Nuclear Instruments and Methods in Physics Research Section B: Beam*  
1395 *Interactions with Materials and Atoms* 268, 790-794.

1396 Salvador, P.G., Berger, J.F., Gauthier, E., Vanniere, B., 2004. Holocene fluctuations of the Rhône River in the  
1397 alluvial plain of the basses terres (Isère, Ain, France). *Quaternaire* 15, 177–186.

1398 Sanderson, D.C.W, Murphy, W., 2010. Using simple portable OSL measurements and laboratory characterisation  
1399 to help understand complex and heterogeneous sediment sequences for luminescence dating. *Quaternary*  
1400 *Geochronology* 5, 299–305.

1401 Santonja, M., Pérez-González, A., Domínguez-Rodrigo, M., Panera, J., Rubio-Jara, S., Sesé, C., Soto, E., Arnold,  
1402 L. J., Duval, M., Demuro, M., Ortiz, J.E., de Torres, T., Mercier, N., Barba, R., Yravedra, J., 2014. The Middle  
1403 Paleolithic site of Cuesta de la Bajada (Teruel, Spain): a perspective on the Acheulean and Middle Paleolithic  
1404 technocomplexes in Europe. *Journal of Archaeological Science* 49, 556-571.

1405 Schaefer, J.M., Faestermann, T., Herzog, G.F., Knie, K., Korschinek, G., Masarik, J., Meier, A., Poutivtsev, M.,  
1406 Rugel, G., Schlüchter, C., Serifiddin, F., Winckler, G., 2006. Terrestrial manganese-53 - A new monitor of Earth  
1407 surface processes. *Earth and Planetary Science Letters* 251, 334–345.

1408 Scherbina, O. I. and Brik, A. B., 2000. Temperature stability of carbonate groups in tooth enamel. *Applied*  
1409 *Radiation and Isotopes* 52, 1071-1075.

1410 Schmidt C., Kreuzer S., DeWitt R., Fuchs M., 2015. Radiofluorescence of quartz : a review. *Quaternary*  
1411 *Geochronology* 27, 66-77.

1412 Schmidt, S., Hetzel, R., Kuhlmann, J., Mingorance, F., Ramos, V.A., 2011. A note of caution on the use of  
1413 boulders for exposure dating of depositional surfaces. *Earth and Planetary Science Letters* 302, 60–70.

1414 Scholz, D., Hoffmann, D.L., 2008.  $^{230}\text{Th}/\text{U}$ -dating of fossil reef corals and speleothems. *Eiszeitalter und*  
1415 *Gegenwart – Quaternary Science Journal* 57, 52-77.

1416 Schramm, A., Stein, M., Goldstein, S.L., 2000. Calibration of the  $^{14}\text{C}$  time scale to >40 ka by  $^{234}\text{U}$ - $^{230}\text{Th}$  dating of  
1417 Lake Lisan sediments (last glacial Dead Sea). *Earth and Planetary Science Letters* 175, 27-40.

1418 Schreve, D.C., 2001. Differentiation of the British late Middle Pleistocene interglacials: the evidence from  
1419 mammalian biostratigraphy. *Quaternary Science Reviews* 20, 1693-1705.

1420 Schreve, D.C., Keen, D.H., Limondin-Lozouet, N., Auguste, P., Santistebane, J.I., Ubilla, M., Matoshko, A.,  
1421 Bridgland, D.R., Westaway, R., 2007. Progress in faunal correlation of Late Cenozoic fluvial sequences 2000–4:  
1422 the report of the IGCP 449 biostratigraphy subgroup. *Quaternary Science Reviews* 26, 2970-2995.

1423 Schulte, L., Julià, R., Burjachs, F., Hilgers, A., 2008. Middle Pleistocene to Holocene geochronology of the River  
1424 Aguas terrace sequence (Iberian Peninsula): Fluvial response to Mediterranean environmental change.  
1425 *Geomorphology* 98, 13-33.

1426 Schwarcz, H.P., 1989. Uranium series dating of Quaternary deposits. *Quaternary International* 1, 7-17.

1427 Schwarcz, H.P., Latham, A. G., 1989. Dirty calcites 1. Uranium-series dating of contaminated calcite using  
1428 leachates alone. *Chemical Geology* 80, 35-43.

1429 Sharp, W.D., Ludwig, K.R., Chadwick, O.A., Amundson, R., Glaser, L.L., 2003. Dating fluvial terraces by  $^{230}\text{Th}/\text{U}$   
1430 on pedogenic carbonate, Wind River Basin, Wyoming. *Quaternary Research* 59, 139-150.

1431 Siame, L.L., Bournès, D.L., Sébrier, M., Bellier, O., Carlos Castano, J., Araujo, M., Perez, M., Raisbeck, G.M.,  
1432 Yiou, F., 1997. Cosmogenic dating ranging from 20 to 700 ka of a series of alluvial fan surfaces affected by the El  
1433 Tigre fault, Argentina. *Geology* 25, 975-978.

1434 Singareya, J.S., Bailey, R.M., 2004. Component-resolved bleaching spectra of quartz optically stimulated  
1435 luminescence: preliminary results and implications for dating. *Radiation Measurements* 38, 111–118.

1436 Stock, G.M., Anderson, R.S., Finkel, R.C., 2004. Pace of landscape evolution in the Sierra Nevada, California,  
1437 revealed by cosmogenic dating of cave sediments. *Geology* 32, 193-196.

1438 Stokes, S., Bray, H.E., Blum, M.D., 2001. Optical resetting in large drainage basins: tests of zeroing assumptions  
1439 using single-aliquot procedures. *Quaternary Science Reviews* 20, 879-885.

1440 Stone, A.E.C., Bateman, M.D., Thomas, D.S.G., 2015. Rapid age assessment in the Namib Sand Sea using a  
1441 portable luminescence reader. *Quaternary Geochronology* 30, 134-140.

1442 Stuiver, M., Polach, H.A., 1977. Discussion; reporting of C-14 data. *Radiocarbon* 19, 355-363.

1443 Thomsen, K.J., Murray, A.S., Jain, M., Bøtter-Jensen, L., 2008. Laboratory fading rates of various luminescence  
1444 signals from feldspar-rich sediment extracts. *Radiation measurements* 43, 1474-1486.

1445 Thomsen, K.J., Murray, A.S., Jain, M., 2012. The dose dependency of the overdispersion of quartz OSL single  
1446 grain dose distributions. *Radiation Measurements* 47, 732-739.

1447 Tissoux, H., Falguères, C., Voinchet, P., Toyoda, S., Bahain, J.-J., Despriée, J., 2007. Potential use of Ti-center  
1448 in ESR dating of fluvial sediment. *Quaternary Geochronology* 2, 367-372.

1449 Tissoux, H., 2015. Sediment, ESR. *Encyclopedia of Scientific Dating Methods*. J. W. Rink and J. Thompson.  
1450 Dordrecht, Springer Netherlands, 743-747.

1451 Torfstein, A., Goldstein, S.L., Kagan, E J., Stein, M., 2013. Integrated multi-site U-Th chronology of the last glacial  
1452 Lake Lisan. *Geochimica et Cosmochimica Acta* 104, 210-231.

1453 Toyoda, S., Voinchet, P., Falguères, C., Dolo, J.M., Laurent, M., 2000. Bleaching of ESR signals by the sunlight:  
1454 a laboratory experiment for establishing the ESR dating of sediments. *Applied Radiation and Isotopes* 52, 1357-  
1455 1362.

1456 Toyoda, S., 2015. Paramagnetic lattice defects in quartz for applications to ESR dating. *Quaternary  
1457 Geochronology* 30, 498-505.

1458 Turney, C.S., Coope, G.R., Harkness, D.D., Lowe, J.J., Walker, M.J., 2000. Implications for the dating of  
1459 Wisconsinan (Weichselian) Late-Glacial events of systematic radiocarbon age differences between terrestrial  
1460 plant macrofossils from a site in SW Ireland. *Quaternary Research* 53, 114-121.

1461 Vandenberghe, J., Gracheva, R., Sorokin, A., 2010. Postglacial floodplain development and Mesolithic-Neolithic  
1462 occupation in the Russian forest zone. *Proceedings of the Geologists' Association* 121, 229-237.

1463 van der Schriek, T., Passmore, D.G., Franco Mugica, F., Stevenson, A.C., Boomer, I., Rolao, J., 2008. Holocene  
1464 palaeoecology and floodplain evolution of the Muge tributary, Lower Tagus Basin, Portugal. *Quaternary  
1465 International* 189, 135-151.

1466 Van Der Woerd, J., Ryerson, F.J., Tapponnier, P., Gaudemer, Y., Finkel, R., Meriaux, A.S., Caffee, M., 1998.  
1467 Holocene left-slip rate determined by cosmogenic surface dating on the Xidatan segment of the K'unlun fault  
1468 (Qinghai, China). *Geology* 26, 695-698.

1469 Veldkamp, A., Kroonenberg, S., Heijnis, H., Ven den Berg van Saparoea, R., 2004. The suitability of dated  
1470 travertines as a record of fluvial incision: Allier (France) floodplain dynamics during the late Quaternary.  
1471 *Quaternaire* 15, 159-165.

1472 Vis, G.J., Kasse, C., Kroon, D., Jung, S., Zuur, H., Prick, A., 2010. Late Holocene sedimentary changes in  
1473 floodplain and shelf environments of the Tagus River (Portugal). *Proceedings of the Geologists' Association* 121,  
1474 203-217.

1475 Voinchet, P., Bahain, J.J., Falguères, C., Laurent, M., Dolo, J.M., Despriée, J., Gageonnet, R., Chaussé, C.,  
1476 2004. ESR dating of quartz extracted from Quaternary sediments application to fluvial terraces system of northern  
1477 France. *Quaternaire* 15, 135–141.

1478 Voinchet, P., Falguères, C., Tissoux, H., Bahain, J.-J., Despriée, J., Pirouelle, F., 2007. ESR dating of fluvial  
1479 quartz: Estimate of the minimal distance transport required for getting a maximum optical bleaching. *Quaternary*  
1480 *Geochronology* 2, 363-366.

1481 Voinchet, P., Toyoda, S., Falguères, C., Hernandez, M., Tissoux, H., Moreno, D., Bahain, J.J., 2015. Evaluation  
1482 of ESR residual dose in quartz modern samples, an investigation on environmental dependence. *Quaternary*  
1483 *Geochronology* 30, 506-512.

1484 Wallinga, J., 2002. Optically stimulated luminescence dating of fluvial deposits: a review. *Boreas* 31, 303-322.

1485 Wallinga, J., Murray, A.S., Duller, G.A., Törnqvist, T.E., 2001. Testing optically stimulated luminescence dating of  
1486 sand-sized quartz and feldspar from fluvial deposits. *Earth and Planetary Science Letters* 193, 617-630.

1487 Wang, X.L., Lu, Y.C., Wintle, A.G., 2006. Recuperated OSL dating of fine-grained quartz in Chinese loess.  
1488 *Quaternary Geochronology* 1, 89-100.

1489 Wang, X., Van Balen, R., Yi, S., Vandenberghe, J., Lu, H., 2014. Differential tectonic movements in the  
1490 confluence area of the Huang Shui and Huang He rivers (Yellow River), NE Tibetan Plateau, as inferred from  
1491 fluvial terrace positions. *Boreas* 43, 469–484.

1492 Wedepohl, H.K., 1995. The composition of the continental crust. *Geochimica et Cosmochimica Acta* 59, 1217-  
1493 1232.

1494 Wenz, S., Scholz, D., Sürmelihindi, G., Passchier, C.W., Jochum, K.P., Andreae, M.O., 2016. <sup>230</sup>Th/U-dating of  
1495 carbonate deposits from ancient aqueducts. *Quaternary Geochronology* 32, 40-52.

1496 Wintle, A.G., 1973. Anomalous fading of thermoluminescence in mineral samples. *Nature* 245, 143-144.

1497 Wintle A.G., Murray, A.S., 2006. A review of quartz optically stimulated luminescence characteristics and their  
1498 relevance in single-aliquot regeneration dating protocols. *Radiation Measurements* 41, 369-391.

1499 Wolf, D., Seim, A., Faust, D., 2014. Fluvial system response to external forcing and human impact - Late  
1500 Pleistocene and Holocene fluvial dynamics of the lower Guadalete River in western Andalucía (Spain). *Boreas* 43,  
1501 422–449.

1502 Yang, Q., Scholz, D., Jochum, K.P., Hoffmann, D.L., Stoll, B., Weis, U., Schwager, B., Andreae, M.O., 2015. Lead  
1503 isotope variability in speleothems - A promising new proxy for hydrological change? First results from a stalagmite  
1504 from western Germany. *Chemical Geology* 396, 143-151.

1505 Zermano, P., Kurdyla, D.K., Buchoilz, B.A., Heller, S.J., Kashgarian, M. Frantz, B.R., 2004. Prevention and  
1506 removal of elevated radiocarbon contamination in the LLNL/CAMS natural radiocarbon sample preparation  
1507 laboratory. *Nuclear Instruments and Methods in Physics Research B* 223–224, 293–297.

1508 Zielhofer, C., Faust, D., 2008. Mid- and Late-Holocene fluvial chronology of Tunisia. *Quaternary Science Reviews*  
1509 27, 580-588.

1510 Zhu, S., Wu, Z., Zhao, X., Li, J., Xiao, K., 2014. Ages and genesis of terrace flights in the middle reaches of the  
 1511 Yarlung Zangbo River, Tibetan Plateau, China. *Boreas* 43, 485–504.

1512

1513 **Table captions**

1514 Table 1. Case studies published in outcomes relative to former FLAG activities using one (or more)  
 1515 numerical dating methods detailed in the text.

<b>FLAG special</b>	<b>Radiocarbon</b>	<b>Luminescence</b>	<b>ESR</b>	<b><sup>230</sup>Th/U</b>	<b>TCN</b>
<i>Quaternaire</i> 15, <i>Issue 1-2 (2004)</i>	Briant et al.;		Chaussé et al.;		
	Flez and	Jain et al.	Despriée et	Veldkamp et al.	
	Salvador et al.	Mol et al.	Voinchet et		
	Kuzucuoglu et al.		al.		
Mathieu et al.					
<i>Quaternary International</i> 189, <i>Issue 1 (2008)</i>	Fontana et al.				
	Kalicki et al.				
	van der Schriek et				
<i>Geomorphology</i> 98, <i>Issue 3-4 (2008)</i>	de Moor et al.				
<i>Proceedings of the Geologists' Association,</i> 121, <i>Issue 2 (2010)</i>	Coltorti et al.		Lauer et al.		
	Kasse et al.		Martins et al.		
	Vandenberghé et				
	Vis et al.				
<i>Geomorphology,</i> <i>165-166 (2012)</i>			Cordier et al.		Antón et al.
			Cunha et al.		
			Ramos et al.		
<i>Géomorphologie, Relief, Processus, Environnement,</i> <i>Issue 4 (2012)</i>	Le Jeune et al.				
	Piovan et al.				
<i>Boreas</i> 43, <i>Issue 2 (2014)</i>	Wolf et al.		Cordier et al.		Zhu et al.
	Zhu et al.		Wang et al.		
<i>Quaternaire</i> 26, <i>Issue 1 (2015)</i>	Garnier et al.		Harmand et al.		

1516

1517

1518

1519

1520

1521 Table 2. Sampling and laboratory techniques to improve accuracy in radiocarbon dating fluvial  
 1522 deposits. AMS = accelerator mass spectrometry.

Issue	Sampling/laboratory solution
<b>1) Dating suitable material</b>	
<i>Age difference between <sup>14</sup>C dated sediment deposit and the deposit / event for which an age is required</i>	Select samples for dating according to sedimentary context and, where possible, from close to boundaries between sedimentary units (c.f. 'change after' dates (Macklin et al., 2010).
<i>Danger of reworking of fossil material either whole or as organic detritus (e.g. Rogerson et al., 1992)</i>	Date only the identifiable fraction of the deposit – e.g. thoroughly cleaned specific plant macrofossils, shells or bones (e.g. Turney et al., 2000). This is only possible because of AMS techniques which allow dating of small samples.
<i>Danger of field contamination by modern organic detritus</i>	
<b>2) Freshwater reservoir effect</b>	
<i>Danger of carbon uptake from carbonate rich water rich in 'old' carbon</i>	Date only macrofossils from terrestrial species which do not photosynthesise under water (e.g. Carex, Scirpus).
<b>3) Pretreatments to remove contaminants</b>	
<i>Danger of secondary carbonate from post-depositional groundwater infiltration</i>	Dilute HCl pre-treatment (first step of the mild ABA below).
<i>Danger of humic acid infiltration from higher in the profile – especially if overlain by peat</i>	<p>For younger samples (&lt; ~25 <sup>14</sup>C yr BP): mild acid-base-acid (ABA) washes as standard pretreatment</p> <p>For older samples, other pretreatments are recommended to remove more contamination:</p> <ul style="list-style-type: none"> <li>• Ultrafiltration on bone (e.g. Higham et al., 2006)</li> <li>• ABOx-SC (acid, base, wet oxidation - stepped combustion) on charcoal (Bird et al., 1999)</li> <li>• No clear favoured protocols as yet for seeds or shells</li> </ul>
<b>4) General considerations</b>	
<i>Sampling and laboratory preparation.</i>	<ul style="list-style-type: none"> <li>• Ensure laboratory space and all equipment being used for preparation has never previously come into contact with radioactive elements (e.g. from biological researchers using <sup>14</sup>C as a tracer element – Zermeno et al., 2004).</li> <li>• Avoid organic packaging such as paper</li> <li>• Process and store sample in deionised water only</li> <li>• Clean working conditions, avoiding contact of samples or equipment with paper where possible</li> <li>• Powderless laboratory gloves</li> <li>• Visual checks for contamination</li> <li>• Dry samples soon after identification to prevent fungal growth during storage</li> <li>• Submit as large a sample size as possible – preferably &gt;1.4 mg carbon content, i.e. &gt;5 mg dry weight (Brock et al., 2010)</li> </ul>

1523

1524

1525 Table 3. A brief overview of the OSL dating method applied to quartz and feldspar grains extracted  
 1526 from sediment.

	Quartz (SAR)	Quartz (TT-OSL)	Feldspar (IRSL)	Feldspar (pIR-IRSL)
<b>Upper range dating</b>	Present-day			
<b>Lower range dating</b>	200-300 Gy – c. 950 ka i.e. c. 150 ka + (depending on dose rate)		Unclear due to c. 950 ka anomalous fading – c. 300 ka?	
<b>Main strength of the application</b>	Can date fluvial sediments directly. Can date beyond the C-14 dating time range. TT-OSL and pIR-IRSL can extend back to c. 1 Ma			
<b>Standard precision</b>	Standard errors are usually ~10% (5-15%)			

1527

1528

1529

1530 Table 4. A brief overview of the ESR dating method applied to fossil teeth and optically bleached  
 1531 quartz grains extracted from sediment. Further details regarding the dating time range of each  
 1532 application may be found in Duval (2016) and references therein.

	Fossil tooth enamel	Optically bleached quartz grains extracted from sediment
<b>Dated event</b>	Burial of the fossil tooth (usually assumed to happen shortly after the death of the animal).	Last exposure of the sediment to sunlight
<b>Main specificity of the application</b>	Dental tissues are open-systems for U: U-uptake needs to be modeled (combined U-Series/ESR dating approach).	Light-sensitive ESR signals (same basic principles as OSL dating). Presence of a residual (non-bleachable) ESR intensity for the Al centre.
<b>Upper dating range</b>	Present-day	~10 ka
<b>Lower dating range</b>	Early Pleistocene	Miocene (Al-center)
<b>Optimum dating range</b>	40-800 ka	200 ka-2 Ma
<b>Main strength of the application</b>	Direct dating of hominin and animal fossil remains beyond the C-14 and U-series dating time range.	May date beyond the OSL dating time range.
<b>Standard precision</b>	Standard errors are usually ~10% (5-15%)	Standard errors are usually ~10% (5-15%)

1533

1534

1535

1536

1537 Table 5. Summary of the main features usually observed for the three paramagnetic centres Al, Ti-Li  
 1538 and Ti-H. Relative characterisation is provided: (+++)=high, (++)=medium, (+)=low. Further details and  
 1539 additional references may be found in the text.

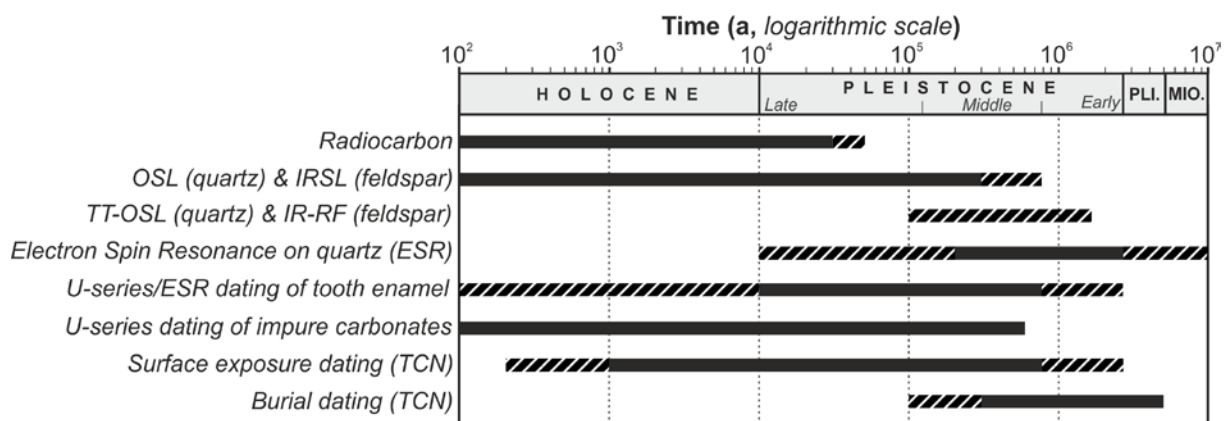
	<i>Al Centre</i>	<i>Ti-Li Centre</i>	<i>Ti-H Centre</i>
<b>Signal-to-Noise (S/N) ratio</b>	+++	++	+
<b>Precision of the measurements</b>	+++	++	+
<b>Dose response curve</b>	No apparent saturation at high doses (>60 kGy)	Non-monotonic behaviour (maximum intensity ~6-10 kGy)	Non-monotonic behaviour (maximum intensity ~3-8 kGy)
<b>Bleaching kinetics (speed)</b>	+	++	+++
<b>Residual ESR intensity (unbleachable component)</b>	Yes	No	No

1540

1541

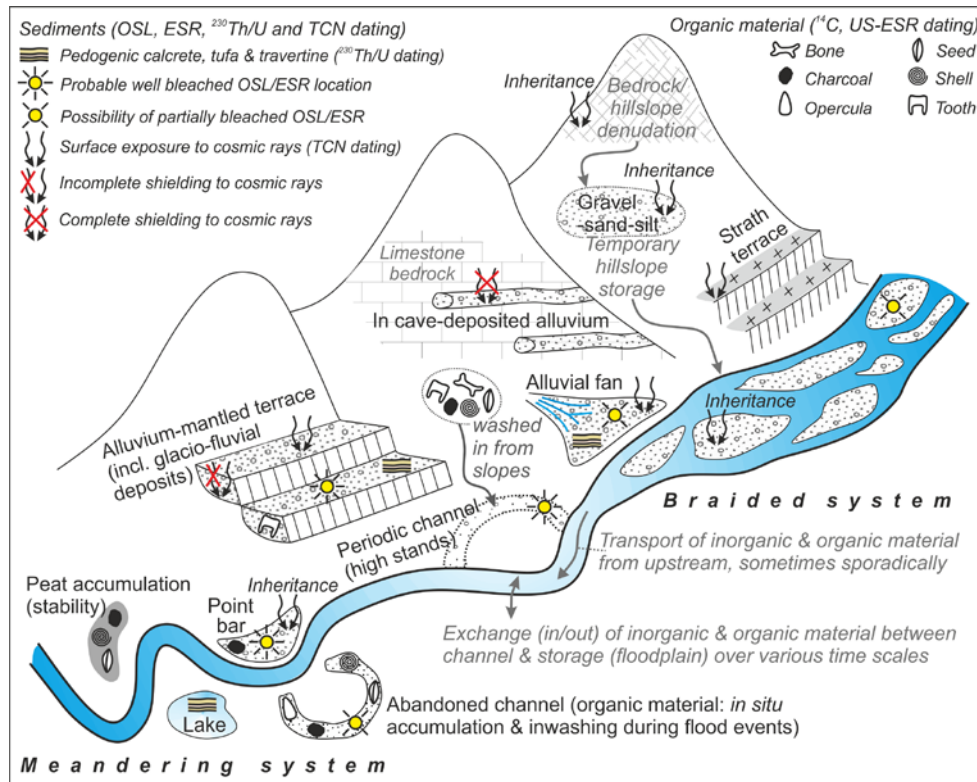
1542 **Figure captions**

1543 Fig. 1. Dateable ranges of the five numerical dating methods detailed in this contribution. Black  
 1544 rectangles refer to time spans within which the methods usually provide reliable results; dashed  
 1545 rectangles represent challenging time periods. Luminescence methods are divided into two rows: the  
 1546 first row represents the routinely applied techniques (OSL: optically stimulated; IRSL: infrared  
 1547 stimulated, including pIRIR) and the second row the techniques currently under development (TT:  
 1548 thermally transferred; RF: radiofluorescence). ESR dating on quartz and U-series/ESR dating of tooth  
 1549 enamel as well as surface exposure dating and burial dating with terrestrial cosmogenic nuclides  
 1550 (TCN) are also divided because of the different dating principles.



1551

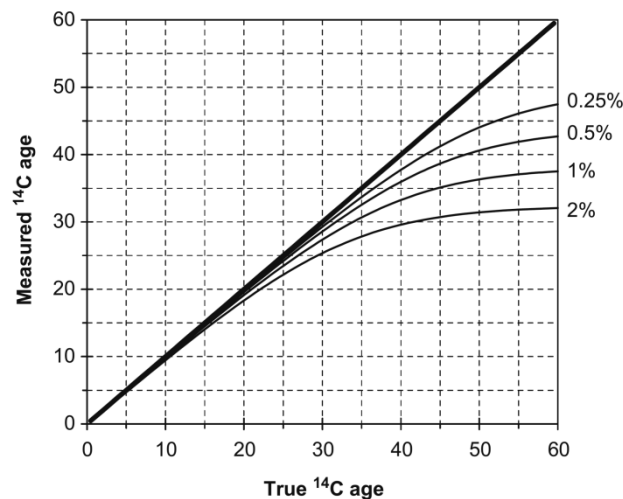
1552 Fig. 2. Sketch representing the dateable deposits/landforms and the pathways of dateable material for  
 1553  $^{14}\text{C}$ , OSL/IRSL, ESR,  $^{230}\text{Th}/\text{U}$  and TCN dating in both braided and meandering fluvial systems.  
 1554 Transport pathways and temporary storages of both inorganic (gravel, sand, silt) and organic (bone,  
 1555 charcoal, opercula, seed, shell and tooth) materials on hillslopes and in the fluvial system are also  
 1556 represented.



1557

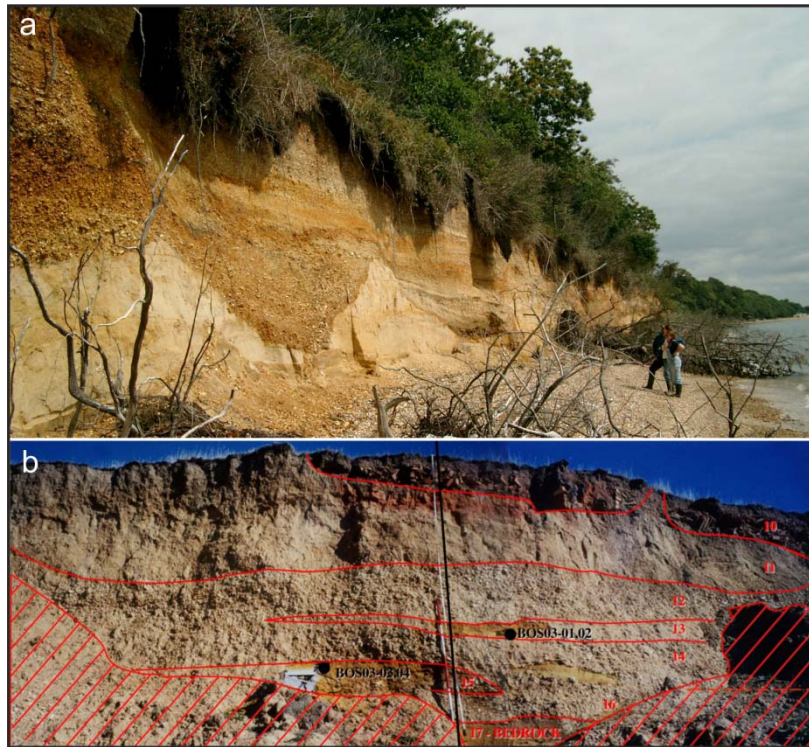
1558

1559 Fig. 3. The impact of modern contamination (0.25–2% by weight) on measured  $^{14}\text{C}$  ages (thin lines)  
 1560 compared to the 1:1 or uncontaminated line (thickest line). After Pigati et al. (2007)



1561

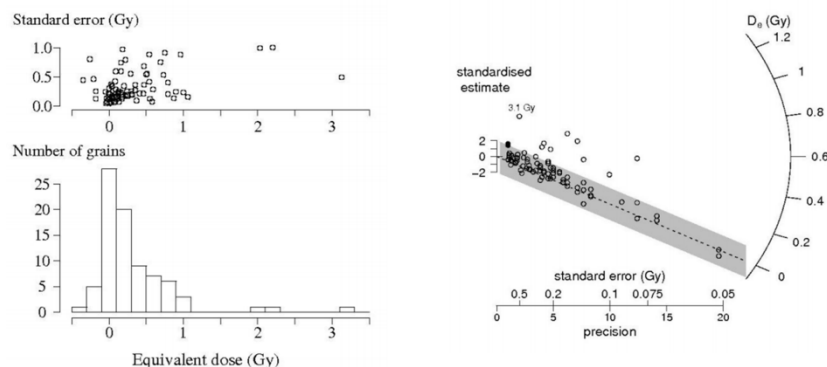
1562 Fig. 4. a) A good sampling location for Luminescence dating at Stanswood Bay, Hampshire, England  
 1563 (Briant et al., 2006). The thickest sand bed at the base is Mesozoic in age, but samples were taken  
 1564 from thick sand beds above the gravel channel (as shown and above the photo out of view). b) Less  
 1565 optimal sampling location for Luminescence dating at Barton on Sea, Hampshire, England (Briant et  
 1566 al., 2006). Field gamma spectrometry was undertaken to mitigate the complex dose rate effect of the  
 1567 thinner sand lenses.



1568

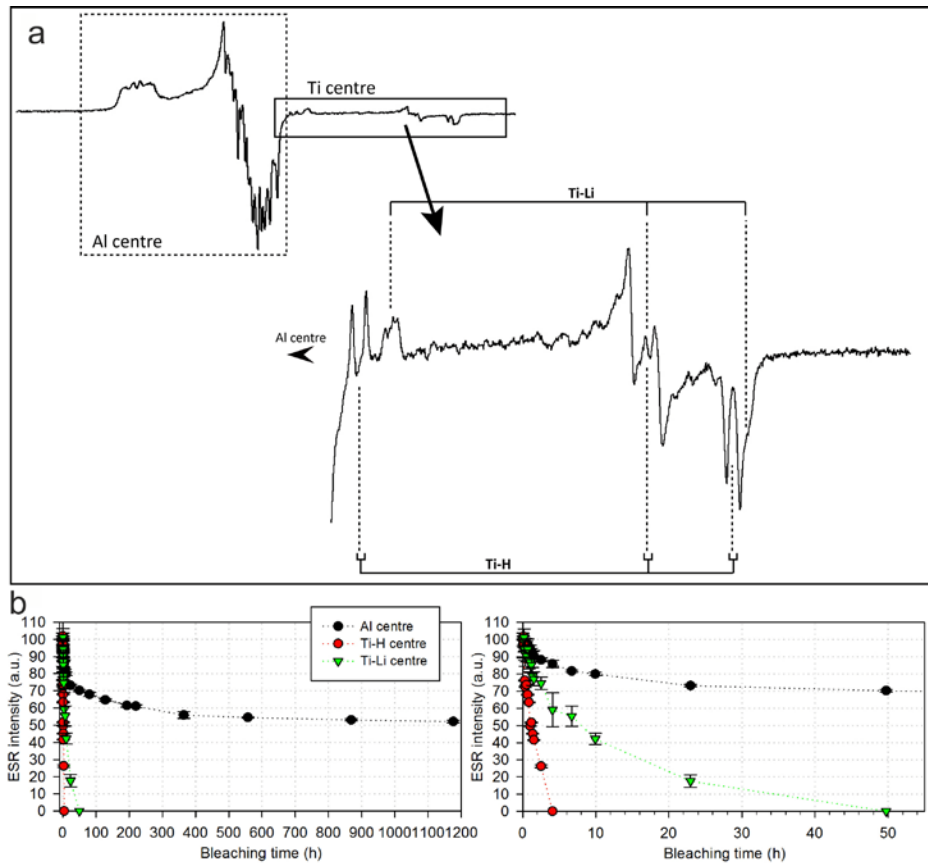
1569

1570 Fig. 5. Comparison of two common methods of plotting data (82 aliquots of aeolian quartz). The radial  
 1571 plot on the right is able to show both precision and equivalent dose on the same plot. This is not  
 1572 possible with the histogram on the left, nor with commonly used probability density plots. Figures 1  
 1573 and 2 of Galbraith (2010).



1574

1575 Fig. 6. a) Examples of ESR spectra of Al and Ti centres measured in quartz. b) Decay of the ESR  
 1576 intensity of the different centres Al, Ti-Li and Ti-H under UV exposure. This laboratory bleaching  
 1577 experiment was performed with a SOL2 sunlight simulator (Dr Hönle) on a quartz sample from the  
 1578 Morée-Villeprovert locality, France.



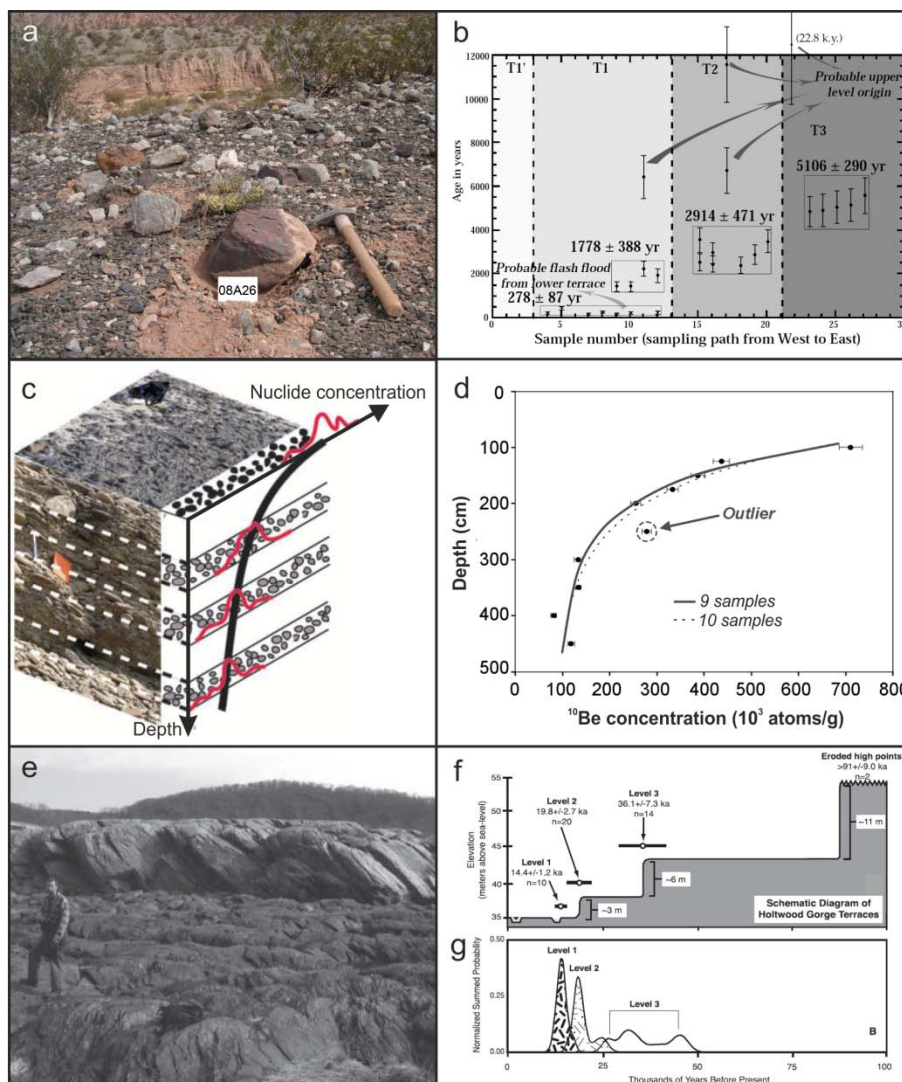
1579

1580

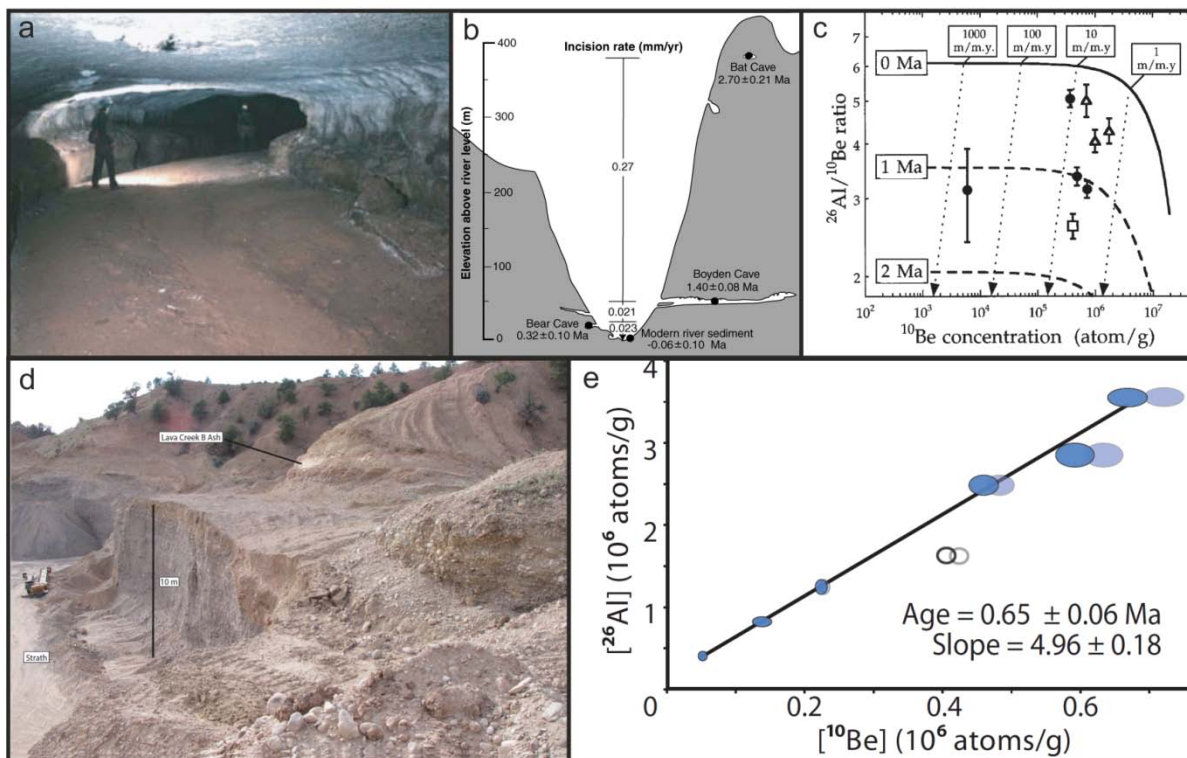
1581

1582 Fig. 7. Surface exposure dating: application of distinct sampling strategies to different fluvial archives  
 1583 or landforms (left), exemplified by dating results (right). a) Sandstone boulder lying at the surface of an  
 1584 alluvial fan, sampled for  $^{10}\text{Be}$  concentration measurement (Escondida creek, Andean Precordillera,  
 1585 Argentina). After Schmidt et al. (2011); b) Mean surface exposure ages (bold numbers), calculated  
 1586 from  $^{10}\text{Be}$  and  $^{26}\text{Al}$  concentration measurements in individual clasts samples, for three fan terraces  
 1587 displaced by Holocene strike-slip faulting activity (NE Tibet). The young age cluster on T1 is attributed  
 1588 to the occurrence of a recent flash flood (light arrow) whereas the four samples from T1, T2 and T3  
 1589 with much older apparent ages (dark arrows) are supposed to have been reworked from older  
 1590 deposits but may also have a higher inherited content. After Van der Woerd et al.(1998); c) Sketch of  
 1591 TCN concentrations along a depth profile (bold black curve) in an alluvial sequence deposited in a

1592 single event, highlighting a concentration decrease with depth. Red curves represent supposed  
 1593 frequency distribution of nuclide concentrations of individual clasts, illustrating the need to  
 1594 amalgamate tens of clasts. Modified after Ivy-Ochs and Kober (2008); d) measured  $^{10}\text{Be}$   
 1595 concentrations with  $1\sigma$  error bars along a  $\sim 4.5$  m-deep profile in terrace sediments (Ourthe river,  
 1596 Ardenne massif, Belgium) and modelled curves based on 10 or 9 samples (bold and dashed curves,  
 1597 respectively). Modified after Rixhon et al. (2011); e) two distinct levels of fluvially-carved strath  
 1598 terraces; both bedrock surfaces were sampled for  $^{10}\text{Be}$  concentration measurements (Susquehanna  
 1599 river, Appalachian mountains, USA). After Reusser et al. (2004); f) Sketch summarizing the Late  
 1600 Pleistocene incision in the Susquehanna river based on  $^{10}\text{Be}$  concentrations of distinct strath terraces  
 1601 (with a minimum age for the upper, strongly eroded surface); g) Normalized cumulative probability  
 1602 curves based on the sample numbers of fig. f for the three lower terrace levels. After Reusser et al.  
 1603 (2006).



1605 Fig. 8. Burial dating: application of two sampling strategies to different fluvial archives (left),  
 1606 exemplified by dating results (right). a) Horizontal, abandoned phreatic tube, partly filled with river  
 1607 sediments (Cumberland river catchment, Appalachian mountains, USA). Note the regular elliptic  
 1608 cross-section of the former phreatic passage. After Anthony and Granger (2007), photo: D. Granger;  
 1609 b) Topographic cross-section across the South Fork river canyon (Sierra Nevada, USA) displaying the  
 1610 multi-level cave system in which burial dating was performed. Note the significant decrease of incision  
 1611 rates toward present. After Stock et al. (2004); c) erosion-burial diagram, the bold line represents the  
 1612  $^{26}\text{Al}/^{10}\text{Be}$  ratio in steadily eroding rocks whereas the dashed curves refer to equal burial duration  
 1613 (dotted lines refer to pre-burial erosion rates). All samples plot beneath the bold line and have  
 1614 therefore experienced burial (New river, Appalachian mountains, USA). After Granger et al. (1997); d)  
 1615 ~10 m-thick, gravel terrace body overlain by a tephra layer, sampled at the base for isochron burial  
 1616 dating because of insufficient shielding to cosmic rays (Gunnison river, Colorado plateau, USA). After  
 1617 Darling et al. (2013), photo: L. Crossey; e) Graphical representation of burial dating isochron for a  
 1618 gravel terrace, the burial age is calculated from the slope of the regression line (Sundays river, South  
 1619 Africa). After Erlanger et al. (2012).



1620

1621

1622

1623 Fig. 9. a) Comparison of  $^{14}\text{C}$  (uncertainties: one standard deviation) and OSL (uncertainties: one  
 1624 standard error) dates. Calibration of radiocarbon dates: Calib 5.0 (Stuiver et al., 2005) with the  
 1625 IntCal04 dataset (Reimer et al., 2004) for ages  $<26$   $^{14}\text{C}$  ka BP and Fairbanks et al. (2005) for ages  $>26$   
 1626  $^{14}\text{C}$  ka BP. Note the systematic age underestimation of  $^{14}\text{C}$  dating beyond the 29-35 ka limit. After  
 1627 Briant and Bateman (2009). b) Plot showing  $^{10}\text{Be}$  depth profile ages and  $^{230}\text{Th}/\text{U}$  ages for alluvial fan  
 1628 deposits, both with  $2\sigma$  error. Shaded red and blue boxes represent the mean  $^{10}\text{Be}$  exposure age and  
 1629 mean U-series age, respectively. Note the slightly younger age range of  $^{230}\text{Th}/\text{U}$  dating (minimum age)  
 1630 than the one defined by the depth profile, proving the usefulness of this combined approach. After  
 1631 Blisniuk et al. (2012). c, d) Integrated  $^{10}\text{Be}$  depth profile and OSL model results in the model  
 1632 parameter space of deposition time ( $t_1$ ), exposure time ( $t_2$ ), and  $^{10}\text{Be}$  inheritance for a single alluvial  
 1633 sequence. The cosmogenic nuclide model best fit (thick red dot) with the 68% confidence level  
 1634 envelope around it (red surface), the OSL model best fit (vertical blue line) with the 68% confidence  
 1635 level envelope around it (blue surface) and the intersection of the two confidence surfaces (dark  
 1636 surface) are shown on (c). The intersection alone is represented on (d), with its 2D projection onto the  
 1637 axial planes (grey surfaces) and further 1D reprojection onto the axes (grey labelled lines). After  
 1638 Guralnik et al. (2011).

